© 2017. Published by The Company of Biologists Ltd | Development (2017) 144, 1045-1055 doi:10.1242/dev.138453

In vitro patterning of pluripotent stem cell-derived intestine recapitulates *in vivo* human development

Yu-Hwai Tsai[1,*], Roy Nattiv[2,3,*], Priya H. Dedhia[1,4], Melinda S. Nagy[1], Alana M. Chin[5], Matthew Thomson[6,‡], Ophir D. Klein[2,3,‡] and Jason R. Spence[1,5,7,‡]

ABSTRACT

The intestine plays a central role in digestion, nutrient absorption and metabolism, with individual regions of the intestine having distinct functional roles. Many examples of region-specific gene expression in the adult intestine are known, but how intestinal regional identity is established during development is a largely unresolved issue. Here, we have identified several genes that are expressed in a region-specific manner in the developing human intestine. Using human embryonic stem cell-derived intestinal organoids, we demonstrate that the duration of exposure to active FGF and WNT signaling controls regional identity. Short-term exposure to FGF4 and CHIR99021 (a GSK3β inhibitor that stabilizes β-catenin) resulted in organoids with gene expression patterns similar to developing human duodenum, whereas longer exposure resulted in organoids similar to ileum. When region-specific organoids were transplanted into immunocompromised mice, duodenum-like organoids and ileum-like organoids retained their regional identity, demonstrating that regional identity of organoids is stable after initial patterning occurs. This work provides insights into the mechanisms that control regional specification of the developing human intestine and provides new tools for basic and translational research.

KEY WORDS: Human, Intestine, Organoid, Patterning, Pluripotent stem cells

INTRODUCTION

The mature gastrointestinal tract is a highly compartmentalized organ with distinct regions that serve specific roles in digestion, absorption, hormone secretion and immunity. Many studies have detailed the complex reciprocal interactions between the endoderm-derived epithelium and the mesoderm-derived stroma for establishing regional identity along the anterior-posterior axis of the gut tube in the early embryo (Dessimoz et al., 2006; Duluc et al., 1994, 2001; Kedinger et al., 1998; Ratineau et al., 2003; Sherwood et al., 2011; Wells and Melton, 2000). However, very little is known about the mechanisms in place after intestinal specification that pattern the duodenum, jejunum and ileum, which make up the regions of the small intestine from proximal to distal.

One of the earliest requirements for intestinal development is the establishment of embryonic posterior identity (Wells and Melton, 1999; Zorn and Wells, 2007). Although the embryo receives anterior-posterior (A-P) positional information prior to and during gastrulation, posterior endoderm identity is not irreversibly specified until after gastrulation (Ho and Kimmel, 1993; Horb and Slack, 2001). At this stage, there are several signaling pathways that promote the posterior patterning of the vertebrate embryo. The WNT and FGF signaling pathways play a central role in establishing the posterior axis of the vertebrate embryo, and Caudal homeobox (Cdx) genes, which are transcription factors that regulate intestinal specification, development and maintenance of regional identity, are targets of these signaling pathways (Beck and Slack, 1999; Beland et al., 2004; Bradley et al., 2000; Cox and Hemmati-Brivanlou, 1995; Dale et al., 1992; Dessimoz et al., 2006; Domingos et al., 2001; Erter et al., 2001; Gao et al., 2009; Grainger et al., 2010; Greco et al., 1996; Gregorieff et al., 2004; Hollyday et al., 1995; Huelsken et al., 2000; Ikeya and Takada, 2001; Isaacs et al., 1998; Keenan et al., 2006; Kiecker and Niehrs, 2001; Lekven et al., 2001; Lickert et al., 2000; Liu et al., 1999; Marvin et al., 2001; McLin et al., 2007; Northrop and Kimelman, 1994; Parr and McMahon, 1995; Pownall et al., 1996; Satoh et al., 2006; Verzi et al., 2010, 2013).

FGF and/or WNT signaling controls posterior fate and intestinal lineage commitment in mouse or human pluripotent stem cells (PSCs) (Cao et al., 2011, 2015; Hannan et al., 2013; Sherwood et al., 2011; Tamminen et al., 2015), and a combination of WNT and FGF signaling can induce an intestinal fate in human definitive endoderm (DE), which gives rise to human intestinal organoids (McCracken et al., 2011; Spence et al., 2011). Although it is clear that hPSC-derived intestinal organoids are small intestinal in identity (Finkbeiner et al., 2015b; Spence et al., 2011; Watson et al., 2014), their exact regional identity (duodenum, jejunum, ileum) is unclear. Here, we sought to clarify the regional identity of organoids, and to determine whether organoids could be patterned into different regions of the intestinal tract. Given that the posterior endoderm of the developing embryo is exposed to higher concentrations and longer durations of growth factors (Arnold and Robertson, 2009), we hypothesized that the duration of exposure to active FGF and WNT signaling would control regional intestinal identity. In this study, we take advantage of hESC-derived intestinal organoids to test this hypothesis. Our results demonstrate that the duration of exposure to active WNT/β-catenin (using CHIR99021, a GSK3β inhibitor) and FGF (FGF4) signaling results in gene and

[1]Department of Internal Medicine, Gastroenterology, University of Michigan Medical School, Ann Arbor, MI 48109, USA. [2]Institute for Human Genetics and Department of Pediatrics, University of California, San Francisco, San Francisco, CA 94143, USA. [3]Program in Craniofacial Biology and Department of Orofacial Sciences, University of California, San Francisco, San Francisco, CA 94143, USA. [4]Department of Surgery, University of Michigan Medical School, Ann Arbor, MI 48109, USA. [5]Department of Cell and Developmental Biology, University of Michigan Medical School, Ann Arbor, MI 48109, USA. [6]Center for Systems and Synthetic Biology, University of California, San Francisco, San Francisco, CA 94143, USA. [7]Center for Organogenesis, University of Michigan Medical School, Ann Arbor, MI 48109, USA.
*These authors contributed equally to this work

‡Authors for correspondence (matthew.thomson@ucsf.edu; ophir.klein@ucsf.edu; spencejr@umich.edu)

J.R.S., 0000-0001-7869-3992

Received 7 April 2016; Accepted 23 November 2016

Development (2017) 144, 1045-1055 doi:10.1242/dev.138453

protein expression profiles that are consistent with tissue that has been patterned into proximal (duodenum) or distal (ileum) small intestine, respectively. To validate our findings, we used both candidate gene expression analysis to compare organoids with the human fetal intestine and an unbiased transcriptome-level approach. To determine whether 'patterned' organoids retain their regional identity *in vivo*, we transplanted organoids into mice, which allows maturation of organoids into adult-like tissue (Finkbeiner et al., 2015b; Watson et al., 2014).

Taken together, our findings shed light on the mechanisms that control regional identity of the developing human intestine. Regionally specified organoids provide a platform for uncovering the genes and signaling pathways that are responsible for common congenital malformations or for functional adaptation of the adult gastrointestinal tract following injury. We suggest that the impact of regional identity is an important consideration in such studies.

RESULTS

Regional identity markers in human fetal intestine

Many genes with differential regional identity in the small intestine have been identified in the adult human and mouse intestine, where gene expression reflects adult region-specific intestinal function, as well as in the developing murine intestine. However, in the developing/fetal human intestine, genes corresponding to adult function are expressed at very low levels (Finkbeiner et al., 2015b), and therefore adult-stage markers do not faithfully identify regional identity in the embryo. Fortunately, several regional identity markers have been described in the fetal mouse intestine (Battle et al., 2008; Dusing et al., 2001; Gao and Kaestner, 2010; Sherwood et al., 2009). To identify a cohort of markers that are regionally expressed in the human intestine, we assessed expression of genes and proteins orthologous to those enriched in embryonic mouse regions by qRT-PCR, *in situ* hybridization and immunofluorescent staining (Fig. 1; n=5, independent biological samples ranging from 14-19 weeks of gestation). Intestines from human fetuses were obtained and divided into thirds, corresponding to the proximal, middle and distal regions of the small intestine. We observed that *PDX1* and *TM4SF4* were enriched in the proximal intestine, similar to the embryonic mouse proximal intestine (Sherwood et al., 2011), whereas the expression of *GATA4* and *ONECUT2* showed non-statistically significant trends of higher expression in the proximal human intestine (Fig. 1A). Of note, some individual samples had more pronounced region-specific expression of *GATA4* and *ONECUT2* when technical replicates were examined (Fig. S1), and regional-specific expression was confirmed for *ONECUT2* using *in situ* hybridization (Fig. 1C), suggesting that region-specific gene expression may be dynamic over time, or may vary significantly between biological specimens; however, additional studies at each time point will be required to more conclusively assess biological variation or time-dependent changes. *Guca2a*, *Osr2*, *Muc2*, *Fzd10*, *Cib2* and several Hox genes have higher distal gene expression levels in mice (Gao and Kaestner, 2010; Sherwood et al., 2009). In the human fetal intestine, *GUCA2A*, *OSR2* and *MUC2* showed increased expression in the distal small intestine (Fig. 1B), along with *HOXB6* (Fig. S1). We confirmed proximal enrichment of PDX1 and *ONECUT2* and distal enrichment of MUC2 and *GUCA2A* using immunofluorescence and *in situ* hybridization (Fig. 1C). Together, these data identify a cohort of molecular markers that are regionally expressed in the human fetal small intestine and demonstrate that some of these regional identifiers are conserved between the mouse and human fetal small intestine.

Prolonged WNT/FGF signaling distalizes hESC-derived intestinal organoids

To examine the effects of WNT and FGF signaling on developing human intestinal tissue, we took advantage of the hESC-derived intestinal organoid culture system (Spence et al., 2011). hESCs were exposed to activin A for 3 days to induce endoderm, which was then exposed to CHIR99021/FGF4-enriched media to induce mid/hindgut spheroid formation, as previously described (Finkbeiner et al., 2015a,b; Xue et al., 2013). Spheroids began to bud from monolayer cultures after 4 days and continuously generated new spheroids for over 10 days; however, incubation beyond 10 days resulted in far fewer spheroids (data not shown). Spheroids were collected from the cultures after 5 days (d5), 7 days (d7) or 10 days (d10), and embedded into matrigel (Fig. 2A). Spheroids were expanded into larger human intestinal organoids for 30-35 days in intestinal growth medium containing EGF, noggin and R-spondin 2 (Fig. 2A). qRT-PCR performed on tissues collected at progressive stages of organoid differentiation, including undifferentiated hESCs, definitive endoderm, hindgut tissue after 4 days of CHIR99021/FGF4 and organoids generated after d5, d7 and d10, showed the expected stage-specific mRNA expression of pluripotency genes (*OCT4*), endoderm genes (*FOXA2*, *SOX17*) and the mid-hindgut and intestinal specification gene *CDX2* (Fig. 2B).

We next evaluated the effects of exposing human DE to CHIR99021 and FGF4 for different lengths of time, and examined the expression of region-specific markers of the developing human intestine identified in Fig. 1. Similar to the human fetal intestine, we found that d5 human organoids had significantly higher expression of the proximal identity marker genes *PDX1*, *TM4SF4*, *GATA4* and *ONECUT2* compared with d7 and d10 organoids (Fig. 2C). Conversely, distally enriched intestinal genes *GUCA2A*, *OSR2* and *MUC2* were expressed at significantly higher levels in d10 organoids compared with d5 and d7 organoids (Fig. 2D). Interestingly, whereas *FZD10* was not regionally expressed in the distal human fetal intestine, it was significantly higher in d10 organoids (Fig. 2D). Although further exploration of this observation is warranted, one possible explanation for this discrepancy is that organoids may represent an earlier stage of development than the human fetal intestine used in this study. Immunostaining confirmed that PDX1 was more abundant in d5 organoids, and that MUC2 was more abundant in d7 and d10 organoids (Fig. 2E).

To further validate our findings, we conducted a series of additional experiments (Fig. S2). We treated endoderm for 5 days with FGF4 plus CHIR99021 (500 ng/ml FGF4, 2 µM CHIR99021), and then varied the concentration of CHIR99021 for the next 5 days, or alternatively, removed CHIR99021 and added IWP2, a WNT inhibitor, or the FGF and ERK inhibitors SU5402 or U0126, respectively (Fig. S2). Spheroids from all conditions were embedded in matrigel and expanded into organoids for 30 days, and were then compared for regional gene expression. As expected, d5 and d10 organoids demonstrated region-specific gene expression when grown in standard conditions (as in Fig. 2, 500 ng/ml FGF4+2µM CHIR99021). However, when CHIR99021 concentrations were reduced, d10 organoids expressed much higher levels of proximal markers but this did not lead to reduced posterior marker gene expression. Interestingly, when WNT signaling was blocked between d5 and d10 (FGF4+IWP2), expression of proximal genes was enhanced and distal gene expression was reduced when compared with d5 and d10 organoids, respectively. These data suggest that, during distalization, one of the roles of WNT/β-catenin may be to repress proximal genes while inducing posterior genes (Fig. S2). In total, these experiments show that prolonged exposure

Development (2017) 144, 1045-1055 doi:10.1242/dev.138453

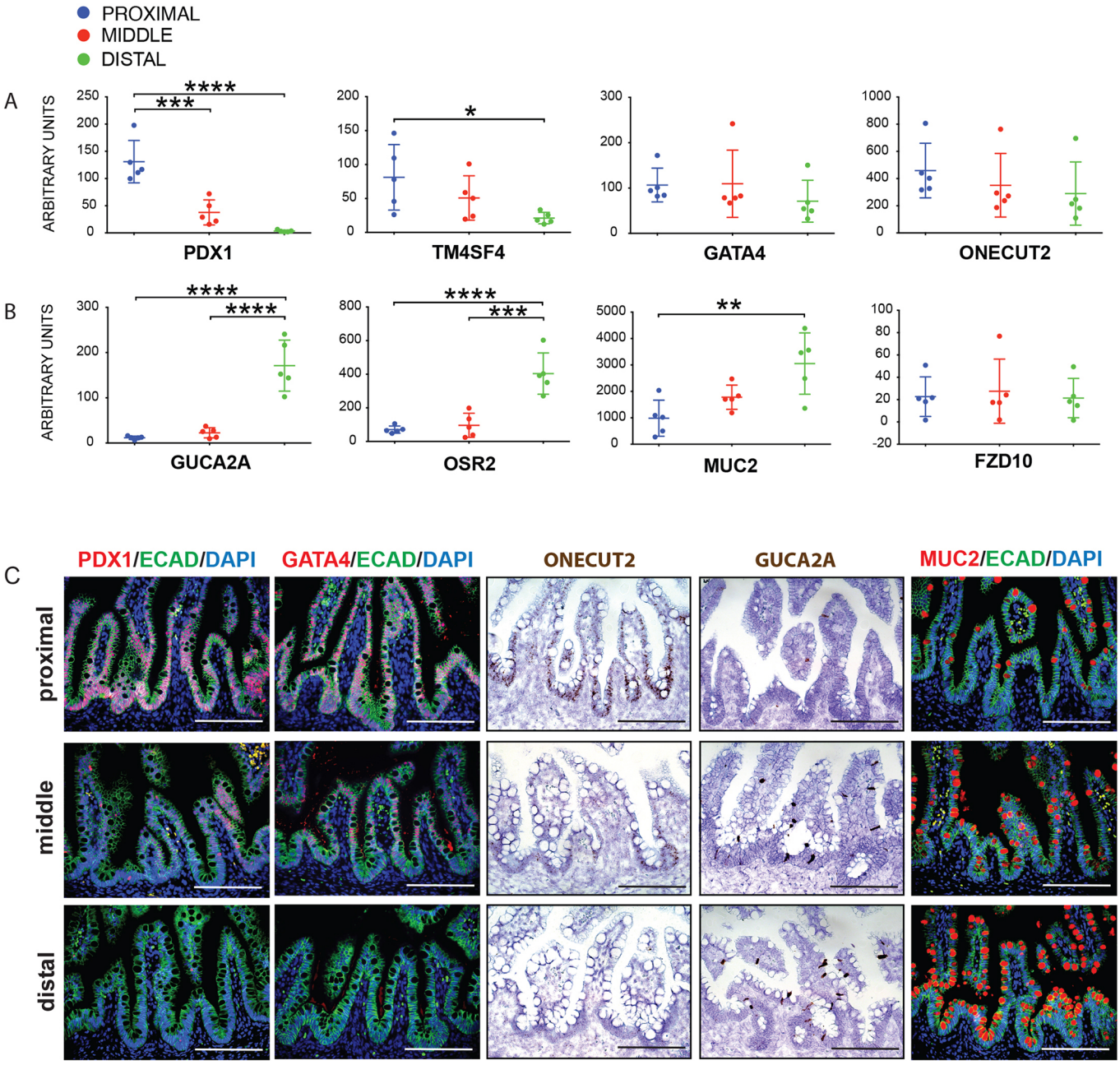

Fig. 1. Identification of regionally expressed molecular markers in the human fetal intestine. (A) Genes known to be enriched in the proximal developing mouse intestine, including *PDX1*, *GATA4*, *TM4SF4* and *ONECUT2* were examined in different regions of the human fetal intestine (*n*=5 individual biological specimens; proximal, blue; middle, red; distal, green). (B) Genes know to be enriched in the distal developing mouse intestine, including *GUCA2A*, *OSR2*, *MUC2* and *FZD10* were examined in different regions of the human fetal intestine (*n*=5 individual biological specimens; proximal, blue; middle, red; distal, green). (C) Enrichment of PDX1 and GATA4 protein as assessed by immunofluorescence and of *ONECUT2* mRNA as assessed by *in situ* hybridization was confirmed in the proximal region of the fetal intestine, whereas *GUCA2A* mRNA and MUC2 protein were enriched in the distal fetal intestine when assessed by *in situ* hybridization and immunofluorescence, respectively. Scale bars: 200 µm.

to high levels of CHIR99021 is required for expression of distal intestinal markers.

Regional identity is maintained over time *in vitro*

It is unclear whether organoids change over time in culture, and it is also unknown whether regional identity might also be determined by the length of time spent in culture. To test this, we generated d5, d7 and d10 organoids, and examined them after 1 month and after 90 days in culture (compare Fig. 2 with Fig. S3). Although some individual regional identity markers changed over time in culture, the trends were similar at the two different time points: d5 organoids had more abundant proximal marker expression with low distal marker expression whereas d10 organoids had low proximal marker expression with enriched distal marker expression.

Whole-transcriptome profiling by RNA sequencing demonstrates that organoids are patterned into proximal and distal intestine

Because the expression patterns of several markers of human fetal proximal-distal intestinal identity suggested that d5 organoids are

Development (2017) 144, 1045-1055 doi:10.1242/dev.138453

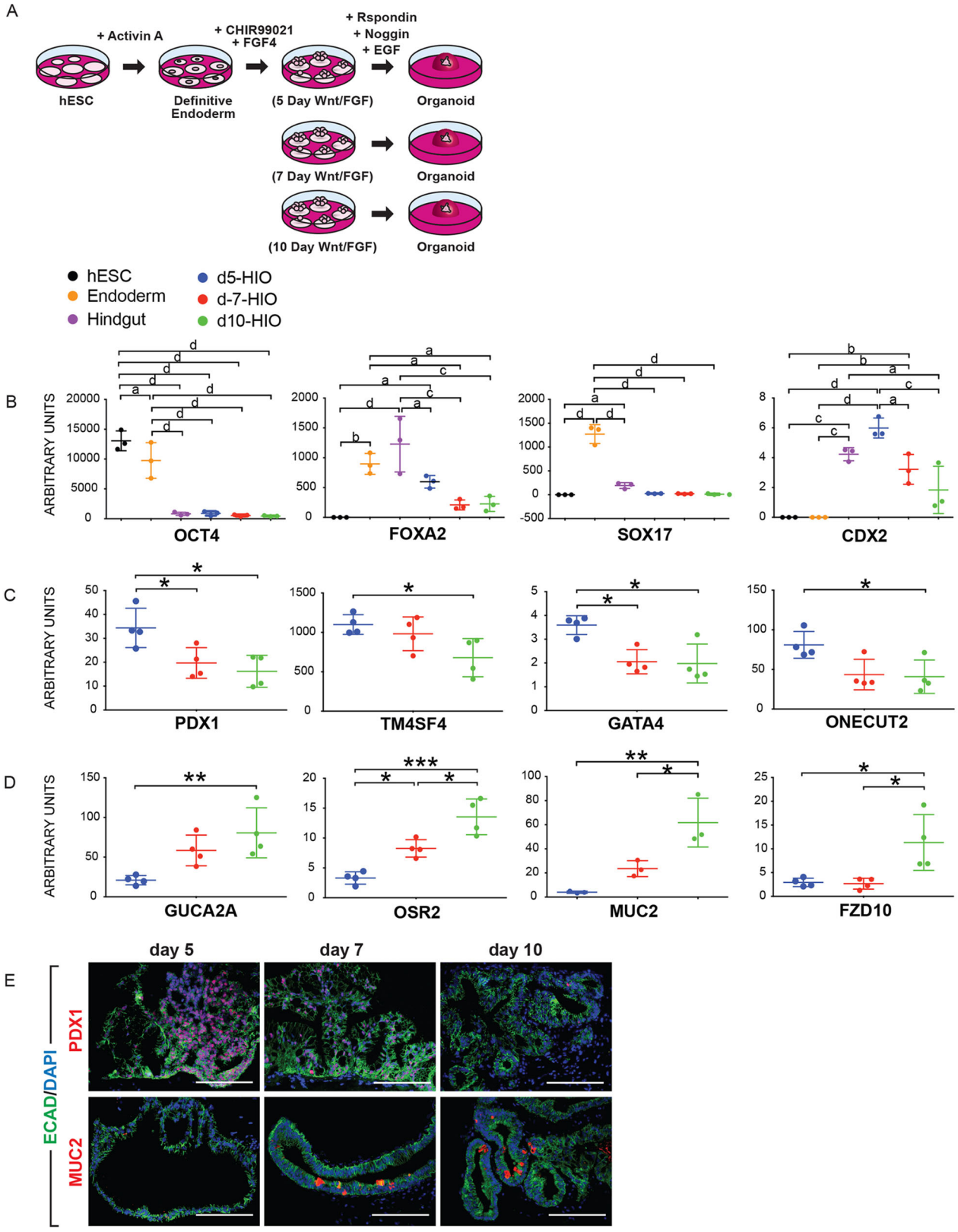

Fig. 2. Human intestinal organoids are patterned by FGF and WNT signaling. (A) Schematic of experimental design showing spheroids generated in culture over increasing periods of time. (B) Expression of *OCT4*, *FOXA2*, *SOX17* and *CDX2* during differentiation in undifferentiated hESCs, in endoderm and hindgut (4 days after FGF4/CHIR99021), and in organoids derived from d5, d7 and d10 cultures (d5, blue; d7, red; d10, green). (C) Markers shown to be enriched in the human fetal duodenum (Fig. 1), including *PDX1*, *GATA4*, *TM4SF4* and *ONECUT2* were examined in d5, d7 and d10 organoids. (D) Markers shown to be enriched in the human fetal ileum (Fig. 1), including *MUC2*, *OSR2*, *MUC2* and *FZD10* were examined in d5, d7 and d10 organoids. (E) Immunofluorescence demonstrated that PDX1 protein expression was enriched in d5 organoids, whereas MUC2 protein expression was enriched in d7 and d10 organoids. Scale bars: 200 µm.

Development (2017) 144, 1045-1055 doi:10.1242/dev.138453

similar to human duodenum and d10 organoids are similar to human fetal ileum (Figs 1 and 2), we next took an unbiased approach to confirm these results. We conducted RNA-sequencing (RNAseq) at different stages of differentiation, including undifferentiated hESCs (H9 hESC line), DE and organoids grown for 30 days from each stage of spheroid formation [5 day organoids (OD5), 7 day organoids (OD7) and 10 day organoids (OD10)].

As a first step towards an unbiased assessment of the hypothesis that d5, d7 and d10 organoids are patterned into proximal or distal intestine, we determined unique stage-specific gene expression patterns in each of our RNAseq datasets. Using non-negative matrix factorization (NNMF) (Brunet et al., 2004), we identified gene expression programs that were highly enriched at one stage among the various conditions (Fig. 3A, Table S1). Each program corresponds to a cohort of genes that are statistically enriched at only one stage. In order to determine whether d5 gene expression programs corresponded to duodenal genes and d7/10 gene expression programs corresponded to ileal genes, we conducted a hypergeometric test to compare organoid gene expression programs (enriched gene sets) against regional identity gene sets of the fetal mouse and human intestine previously identified by microarray (Sherwood et al., 2009; Wang et al., 2015) (Fig. 3B). In this analysis, it was important to compare gene expression programs with data obtained from fetal, as opposed to adult, intestine because, as we have recently demonstrated, organoids resemble fetal intestine and do not express many of the genes found in the adult organ (Finkbeiner et al., 2015b). This analysis revealed that d5 gene sets had statistically significant overlap with genes expressed in the duodenum of the mouse (Sherwood et al., 2009; 'Sherwood duo') and human (Wang et al., 2015; 'Wang duo') ($P<1.0\times10^{-18}$ for both), whereas the d10 gene set had statistically significant overlap with genes expressed in the ileum of the mouse (Sherwood et al., 2009; 'Sherwood ileum'; $P<1.0\times10^{-18}$) and human (Wang et al., 2015; 'Wang ileum'; $P<2.22\times10^{-16}$) (Fig. 3B, Table S2). Importantly, we could not resolve whether d7 organoids are similar to jejunum based on Sherwood et al. and Wang et al., because the gene sets exclusively expressed in this region were very small and did not allow us to perform the statistical comparisons with confidence. Thus, we have limited our conclusions to d5 and d10 organoids. Overlapping genes identified in the duodenum/d5 organoid and ileum/d10 organoids comparisons (Fig. 3B) were further plotted as a heatmap (Fig. 3C). As a control, we also compared d5 and d10 gene expression programs against genes that are enriched in the human fetal colon (Wang et al., 2015). Here, we found no statistically significant overlap, adding confidence to our conclusion that d5 and d10 organoids are most similar to human duodenum and ileum, respectively (Fig. S4).

Confirming regional identity markers in human fetal tissue

The analyses presented thus far demonstrate that increased culture time is well correlated with progressive distalization of intestinal organoids. However, we also needed to grapple with several caveats at this point, including: (1) organoids grown *in vitro* lack many cell types found in the endogenous intestine (e.g. vasculature, enteric neurons, immune cells); (2) genes regionally expressed in the human intestine were identified in tissue grown in culture that supported growth of the epithelium only and that was enriched for stem/progenitor cells but had few differentiated cell types (Wang et al., 2015); and (3) several of the regionally expressed genes were identified in mouse as opposed to human (Sherwood et al., 2009). Therefore, we set out to further validate our findings by investigating expression of genes identified in Fig. 3 (Table S2) in full thickness human fetal intestine. In total, our results had identified 33 'duodenal' genes and 26 'ileal' genes that were consistent across datasets. Of note, several of the genes identified in our unbiased analysis were identified in our candidate approach (Fig. 1), including *PDX1*, *TM4SF4*, *ONECUT2* and *GUCA2A*. We further confirmed that four additional duodenal genes were enriched in the proximal human fetal intestine compared with the distal, and six ileal genes were enriched in the distal compared with the proximal human fetal intestine (Fig. 4, Fig. S5). Although other genes did not show enrichment across the different regions of the human fetal intestine (Figs S6 and S7), it is important to note that examination of technical replicates between intestine regions of individual samples often showed region-specific gene expression (compare Fig. S6 with Fig. S7). Thus, it is possible that our approach has identified additional region-specific markers but that our analysis was not sufficiently powered at individual gestational stages to draw strong conclusions. In addition, it is interesting that many of the genes enriched in the human fetal intestine in a regional manner were regulated in a graded, as opposed to a binary 'on/off', manner, and only a few genes appeared to be expressed exclusively in one region or another.

Regional identity is maintained in patterned organoids transplanted *in vivo*

Organoids grown *in vitro* are similar to the fetal intestine, and upon transplantation into immunocompromised mice, they become more mature at the cellular, molecular and functional levels (Finkbeiner et al., 2015b; Watson et al., 2014). Transplantation also causes morphological remodeling such that the simple epithelium of the organoid *in vitro* gains crypt-villus structure similar to that of the native adult human intestine (Finkbeiner et al., 2015b; Watson et al., 2014). Thus, in order to confirm that the patterned organoids maintained their regional identity when transplanted *in vivo*, we generated d5, d7 and d10 organoids, and transplanted them under the kidney capsule of immunocompromised NSG mice (n=5 per group; Fig. S8). Organoids were allowed to engraft and mature for 10 weeks, and were then harvested for histological and immunohistochemical analysis (Fig. 5, Figs S9 and S10). Low-magnification Hematoxylin and Eosin staining revealed crypt-villus architecture in d5, d7 and d10 transplanted organoids (Fig. 5A, Fig. S9A). As expected, proliferation, marked by Ki67, was restricted to the crypt domains in all transplanted tissues (Fig. S9). In addition, CDX2 and the brush border enzymes sucrose isomaltase (SI) and dipeptidyl peptidase IV (DPPIV), which are expressed throughout the small intestine, were similarly expressed in all regionalized organoids (Fig. S10). By contrast, many proteins known to be expressed in the proximal small intestine (duodenum) were restricted to the d5 organoids, with very little or no expression in d10 organoids (Middendorp et al., 2014; Uhlén et al., 2010), including PDX1, GATA4, FABP2 and LCT (Fig. 5B,C, Fig. S9C). Similarly, proteins previously shown to be enriched in the ileum were more abundant in the d10 organoids, including the transcription factor SATB2, which is expressed at high levels in the adult colon and at lower levels in the distal ileum and FABP6 (Fig. 5D,E) (Uhlén et al., 2010; Wang et al., 2015). In addition, goblet cells, marked by MUC2, were much more abundant in d7 and d10 organoids (Fig. S9E,F).

DISCUSSION

In this study, we provide evidence that the duration of exposure to FGF4 and CHIR99021 is able to specify the regional identity of organoids from human PSCs *in vitro*. This work sheds new light

Development (2017) 144, 1045-1055 doi:10.1242/dev.138453

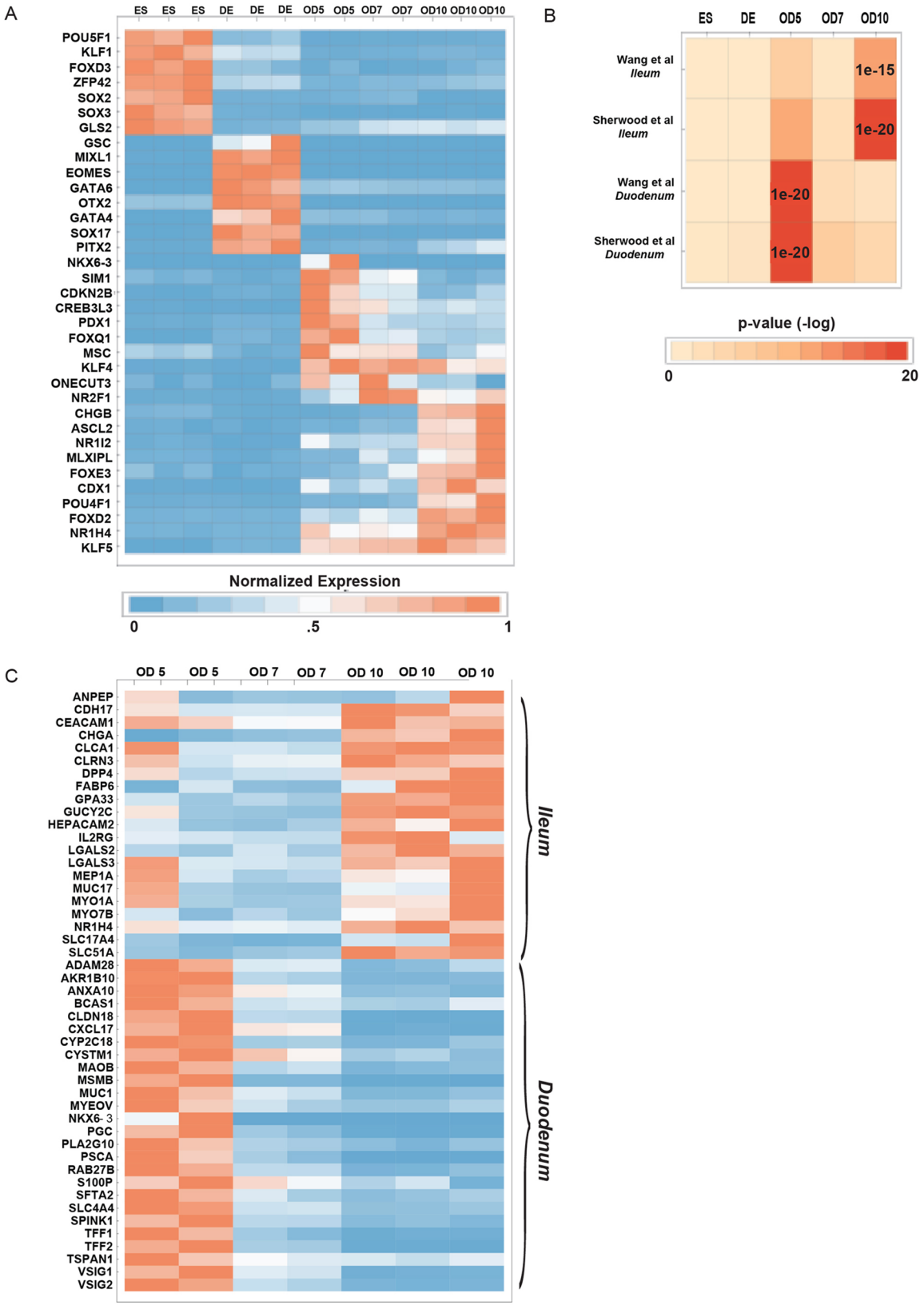

Fig. 3. Bioinformatic identification of stage-enriched genes and comparison with published datasets. (A) Non-negative matrix factorization was used to identify stage-enriched genes. A normalized and curated heatmap shows representative genes (the full list is in Table S1). ES, human embryonic stem cells; DE, definitive endoderm; OD5, day 5 organoids; OD7, day 7 organoids; OD10, day 10 organoids. (B) Enriched genes in d5, d7 and d10 organoids were compared with published lists of genes whose expression is regionally restricted to the duodenum or the ileum. A hypergeometric test was used to determine the level of significance of overlapping gene sets. (C) Heatmap of representative genes found to overlap in patterned organoids and in published datasets shows enrichment for ileal genes in d10 organoids and for duodenal genes in d5 organoids.

Development (2017) 144, 1045-1055 doi:10.1242/dev.138453

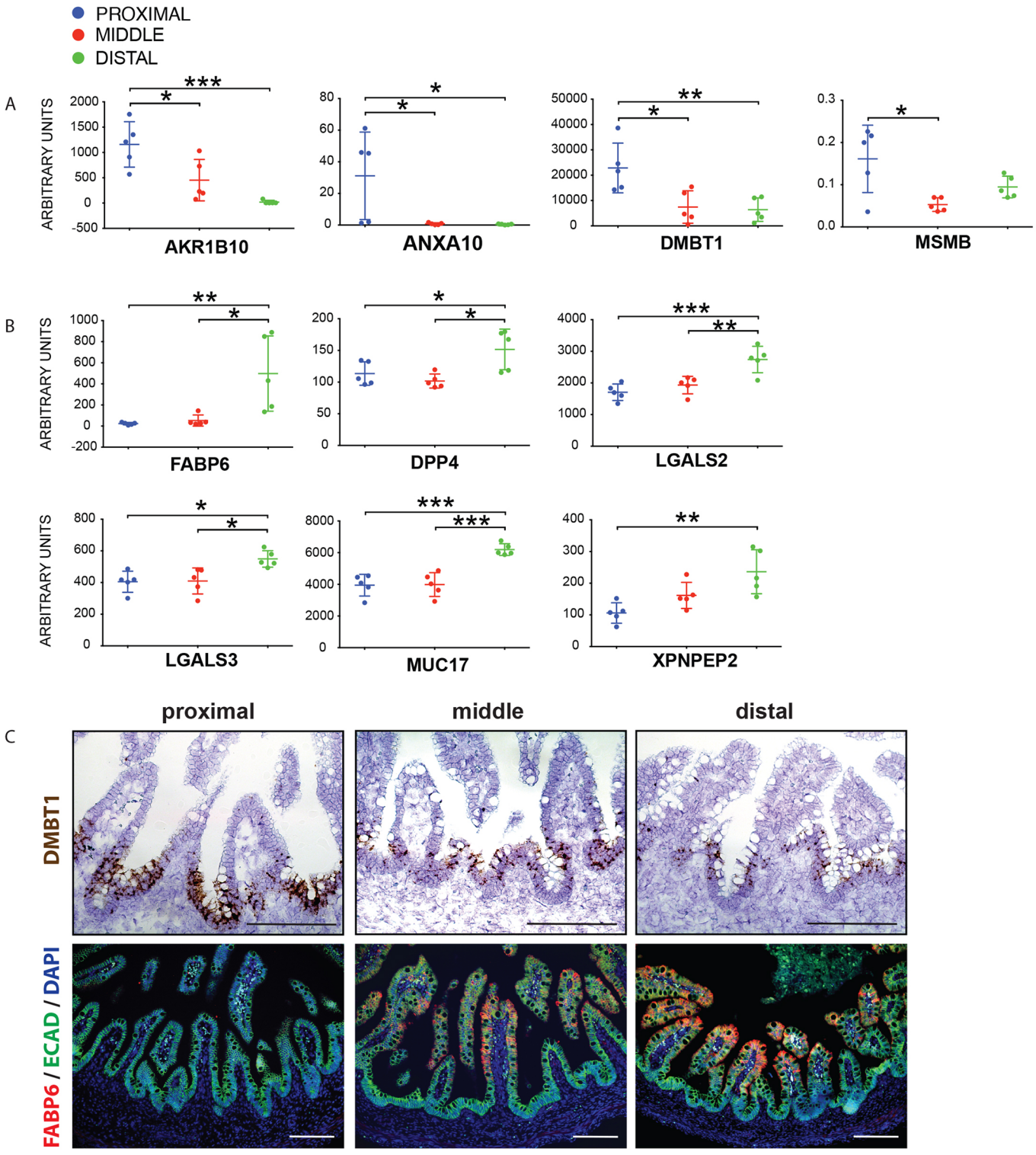

Fig. 4. Validation of region-enriched genes in human fetal tissue. (A) qRT-PCR showing genes enriched in the human fetal proximal small intestine (*n*=5 individual biological specimens; proximal, blue; middle, red; distal, green). (B) qRT-PCR showing genes enriched in the human fetal distal small intestine. (C) *In situ* hybridization of *DMBT1* showing stronger expression in the proximal small intestine, and immunohistochemistry of FABP6 showing more abundant protein staining in the middle/distal regions of the human small intestine. Scale bars: 200 µm.

onto the regional identify of intestinal organoids grown using published methods (Finkbeiner et al., 2015b; McCracken et al., 2011; Spence et al., 2011; Watson et al., 2014), as it has been unclear whether these most closely represented a specific region of the intestine. Here, we show that organoids used in published work most closely represent duodenum, and we demonstrate that prolonged activation of FGF and WNT signaling patterns the intestine into increasingly distal tissue. The notion that duration of exposure to signaling pathway activation can influence identity came from our understanding that, as the embryo develops, the most

Development (2017) 144, 1045-1055 doi:10.1242/dev.138453

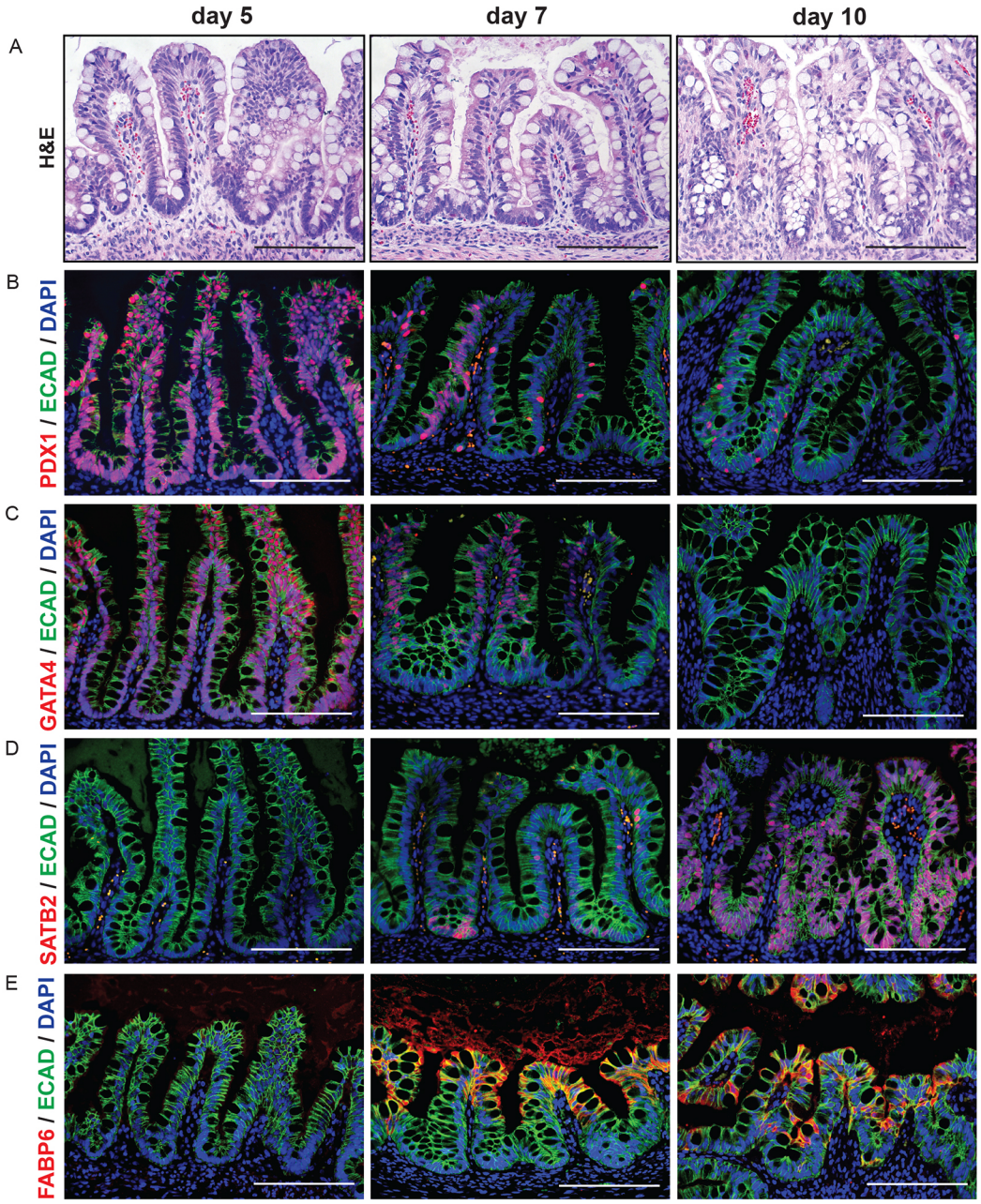

Fig. 5. Organoids retain regionalization after maturation *in vivo*. (A) d5, d7, d10 organoids were harvested after maturation *in vivo*. Hematoxylin and Eosin staining reveals that transplanted tissue possesses villus- and crypt-like domains. (B) PDX1 is most highly enriched in d5 organoids. (C) GATA4 is most highly enriched in d5 organoids. (D) SATB2 is most highly enriched in d10 organoids. (E) FABP6 is enriched in both d7 and d10 organoids. Scale bars: 200 µm.

caudal region of the embryo is exposed to higher levels of growth factor signaling relative to more proximal regions, and that this signaling is prolonged as high concentrations of ligands are maintained distally as the embryonic axis lengthens (Arnold and Robertson, 2009). However, whether or not intestinal patterning was dependent on growth factor signaling activity and time of exposure was unclear. Our findings provide evidence that variables, including concentration and length of exposure, are important for establishing intestinal regional identity.

Furthermore, the current studies also address several practical issues that arise from working with *in vitro*-derived tissues. One important issue that our work raises relates to understanding the strengths and limitations of different organoid model systems in order to ensure that they are employed in the correct context (Chen et al., 2014; Finkbeiner et al., 2015b, 2012; Leslie et al., 2014; Rodansky et al., 2015; Watson et al., 2014; Xue et al., 2013). For example, a number of reports have demonstrated that hPSC-derived organoids are small intestinal in nature and contain Paneth cells (Finkbeiner et al., 2015a,b; Spence et al., 2011; Watson et al., 2014), which are not present in the colon (Rothenberg et al., 2012). However, the regional identity of organoids generated using the same or similar methods to ours has been confused in other research, including recent reports stating that organoids are tissues 'resembling human proximal colon' (Engevik et al., 2015a,b). The current work underscores the observation that organoids, as originally described (Spence et al., 2011), are most similar to duodenum.

Development (2017) 144, 1045-1055 doi:10.1242/dev.138453

In addition to clarifying the nature of these *in vitro*-derived models, another important implication of the current work is the ability to begin generating different regions of the intestine for specific purposes. For example, a dangerous condition in human neonates called necrotizing enterocolitis (NEC) most often affects the ileum. When using organoids to model diseases such as NEC *in vitro*, or for generating tissue engineered small intestine for therapeutic purposes, it will be important to generate organoids that best match the appropriate region of the intestine (Finkbeiner et al., 2015a; Howell and Wells, 2011; Levin et al., 2013; Ullrich et al., 2012).

Given the inability to functionally explore developmental processes in human fetal tissue, using organoids as a surrogate model for human intestine development provides a path for better understanding of the developmental cues responsible for human fetal intestinal regionalization. Previously, little to nothing was known about this process in the human; this study provides the first evidence that the combined signaling activity of FGF and WNT plays a role in establishing regional intestinal identity. In the future, *in vitro*-derived regionalized small intestinal organoids can be used to study specific gene expressions programs and to better understand genes that play important roles in the development of congenital intestinal disease. From a regenerative medicine perspective, regionalized organoids will provide more reliable building blocks for replacement purposes.

MATERIALS AND METHODS

hESC lines, human tissue and mice

hESCs

All work with hESCs was reviewed and approved by the University of Michigan human pluripotent stem cell research oversight committee (HPSCRO). The hESC cell line H9 (WA09, NIH stem registry #0062) was obtained from the WiCell Research Institute. Karyotypically normal cell lines were used for all experiments.

Human tissue

Normal, de-identified human intestinal tissue was obtained from the University of Washington Laboratory of Developmental Biology, and was approved by the University of Michigan institutional review board.

Animal use

All mouse work was reviewed and approved by the University of Michigan Committee on Use and Care of Animals (UCUCA).

Differentiation of hESCs

Differentiation of hESCs and organoids was carried out as previously published, with minor modifications (Finkbeiner et al., 2015b; Leslie et al., 2014; McCracken et al., 2011). In brief, endoderm was generated by adding activin A (100 ng/ml) for 3 consecutive days in Roswell Park Memorial Institute 1640 (RPMI-1640) media supplemented with 0%, 0.2% and 2.0% HyClone FBS. FGF4 (500 ng/ml) plus CHIR99021 (2 µM) were then added to endoderm cultures and medium was replaced daily for 10 days. In our original protocol, spheroids were collected on d4 (McCracken et al., 2011; Spence et al., 2011), whereas in the current work, spheroids were collected on d5, d7 and d10, embedded in matrigel and overlaid with growth medium, as previously described (Finkbeiner et al., 2015b), containing RSPO2-conditioned medium (Bell et al., 2008), noggin-conditioned medium (Heijmans et al., 2013) and EGF. All experiments were conducted on organoids expanded for 30-35 days *in vitro*.

qRT-PCR

Briefly, RNA isolation was performed using MagMAX^{TM}-96 Total RNA Isolation Kit (Ambion, AM1830). A SuperScript VILO cDNA synthesis kit (ThermoFisher, 11754250) was used to make cDNA from 200 ng RNA. cDNA levels were detected using QuantiTect SYBR Green (Qiagen, 608056). Relative gene expression was plotted as Arbitrary Units, using the following formula: [2^(housekeeping gene Ct-gene Ct)]×10,000. All primers sequences are listed in Table S3.

Histology, immunofluorescence and *in situ* hybridization

Immunofluorescence was carried out as previously described (Dye et al., 2015; Rockich et al., 2013) using antibodies outlined in Table S4. *In situ* hybridization was performed using the RNAscope 2.0 HD detection kit, and with commercially available mRNA probes outlined in Table S4, according to the standard protocol provided. All incubations were performed at 40°C in a HybEZ hybridization system oven (Advanced Cell Diagnostics, 310010). All immunostaining or *in situ* hybridization was conducted on at least three independent biological specimens (three independent human fetal samples or three independent organoids), and immunostaining images shown in the figures are representative images unless otherwise noted in the text.

Statistical analysis

For statistical analysis, data are expressed as the median of each sample set. Each data point in the plots represents an independent biological sample. For organoid experiments, each independent biological sample is comprised of three to five organoids pooled together. All organoid experiments were conducted on at least three independent biological replicates, and each experiment was repeated on at least two separate occasions (independent experiments). For human fetal tissue, all analysis was conducted on five independent biological replicates. One-way ANOVA was used for statistical analysis, except for Fig. S2, which used an unpaired *t*-test. Analyses were carried out with GraphPad Prism 5.0 software. Each data point is presented, with the middle line representing the mean, the error bars representing± s.e.m. In all figures, *P<0.05, **P<0.01, ***P<0.001, ****P<0.0001, except for Fig. 2B where a=P<0.05, b=P<0.01, c=P<0.001, d=P<0.0001. For experiments in the supplemental data where individual human fetal samples are plotted (Figs S1, S5, S7), the intestine (n=1 biological sample per time point) was divided into proximal, middle and distal regions, and each region was measured and cut into 1 cm lengths. RNA was isolated from three to five different segments from each of the proximal, middle and distal regions (n=3-5 technical replicates).

RNA sequencing

RNA was isolated directly from tissue culture plates using the MagMAX^{TM}-96 Total RNA Isolation Kit according to the manufacturer's protocol. RNA concentration and purity were assessed using Nanodrop spectrophotometer and bioanalyzed using Agilent RNA 6000 Nano Kit (260/280>1.7 and 260/230>1.7, RIN>8). Samples were stored at −80°C. cDNA libraries were generated using TrueSeq Kit (Illumina). Sequencing was then performed on HiSeq 2000 (Illumina, 100 bp, single-end reads). In all, 42 samples were run using two flow cells and four samples per lane. RNA sequencing data are available in the ArrayExpress database (www.ebi.ac.uk/arrayexpress) under accession number E-MTAB-4168.

RNA sequencing and data analysis

Raw mRNA-seq reads were aligned to hg19 exome constructed from UCSC gff files. Reads were aligned using Bowtie2 v 2.1.0 (Langmead and Salzberg, 2012) with the following options -D 25-R 3-N 1-L 20-i S 1 0.50 local. Transcript counts were normalized to fragments per kilobase of transcript per million mapped reads (FPKM) by applying UCSC transcript lengths and the number of collected reads per sample. Transcripts with a maximum FPKM of less than one across all samples were discarded.

Gene expression programs were assembled using non-negative matrix factorization (Lee and Seung, 1999). Prior to NNMF, the gene expression values were normalized by the mean gene expression value of each gene across all samples. This step removes expression bias and focuses analysis on gene expression variance during the process of differentiation. Following normalization, NNMF was performed both on the entire genome and on DNA-binding proteins as derived through PFAM annotations. DNA-binding proteins provide a reduced set of interpretable genes for comparison with existing literature. NNMF was performed with 10 replicates, and the

Development (2017) 144, 1045-1055 doi:10.1242/dev.138453

highest scoring factorization was selected as the global dictionary of programs.

To assess enrichment of literature gene sets in NNMF programs, gene sets were assembled from Wang et al. (2015) and Sherwood et al. (2009), and gene set enrichment was performed as described previously (Mootha et al., 2003; Subramanian et al., 2005) to determine enrichment in NNMF programs. A gene was determined to be a member of an NNMF-derived program if the gene loading was two standard deviations above the mean loading in the NNMF program. Statistical significance for enrichments was calculated using the hyper-geometric test. Principal component analysis was performed using standard procedures on the FPKM and mean normalized gene expression data.

Kidney capsule transplantation

Kidney capsule transplantation was carried out as previously described (Finkbeiner et al., 2015b; Watson et al., 2014). All organoids were transplanted after being grown *in vitro* for 30-35 days. For each group (d5, d7, d10), organoids were transplanted into five different mice; each transplanted mouse was considered an independent biological specimen (n=5 per group) (Fig. S7). Transplanted organoids were harvested after 10 weeks.

Competing interests

The authors declare no competing or financial interests.

Author contributions

Y.-H.T. and J.R.S. conceived the study. Y.-H.T., R.N., P.H.D., M.S.N., A.M.C. and M.T. conducted experiments. All authors analyzed data. R.N., M.T., O.D.K. and J.R.S. wrote the manuscript. All authors edited and approved final manuscript.

Funding

This research was performed as a project of the Intestinal Stem Cell Consortium – a collaborative research project funded by the National Institute of Diabetes and The National Institute of Diabetes and Digestive and Kidney Diseases (NIDDK) and the National Institute of Allergy and Infectious Diseases (NIAID) (U01DK103141 to J.R.S and U01DK103147 to O.D.K.). This work was also supported, in part, by the NIDDK (K01DK091415), the NIAID (U19AI116482), the University of Michigan Center for Gastrointestinal Research (NIDDK P30DK034933) and the University of Michigan internal funds to J.R.S.; and by RN3 06525 from the California Institute of Regenerative Medicine to O.D.K. The University of Washington Laboratory of Developmental Biology was supported by a National Institutes of Health Award from the Eunice Kennedy Shriver National Institute of Child Health and Human Development (5R24HD000836). Deposited in PMC for immediate release.

Data availability

RNA sequencing data are available in the ArrayExpress database (www.ebi.ac.uk/arrayexpress) under accession number E-MTAB-4168.

Supplementary information

Supplementary information available online at
http://dev.biologists.org/lookup/doi/10.1242/dev.138453.supplemental

References

Arnold, S. J. and Robertson, E. J. (2009). Making a commitment: cell lineage allocation and axis patterning in the early mouse embryo. *Nat. Rev. Mol. Cell Biol.* **10**, 91-103.

Battle, M. A., Bondow, B. J., Iverson, M. A., Adams, S. J., Jandacek, R. J., Tso, P. and Duncan, S. A. (2008). GATA4 is essential for jejunal function in mice. *Gastroenterology* **135**, 1676-1686.e1.

Beck, C. W. and Slack, J. M. (1999). A developmental pathway controlling outgrowth of the Xenopus tail bud. *Development* **126**, 1611-1620.

Beland, M., Pilon, N., Houle, M., Oh, K., Sylvestre, J.-R., Prinos, P. and Lohnes, D. (2004). Cdx1 autoregulation is governed by a novel Cdx1-LEF1 transcription complex. *Mol. Cell. Biol.* **24**, 5028-5038.

Bell, S. M., Schreiner, C. M., Wert, S. E., Mucenski, M. L., Scott, W. J. and Whitsett, J. A. (2008). R-spondin 2 is required for normal laryngeal-tracheal, lung and limb morphogenesis. *Development* **135**, 1049-1058.

Bradley, L., Sun, B., Collins-Racie, L., LaVallie, E., McCoy, J. and Sive, H. (2000). Different activities of the frizzled-related proteins frzb2 and sizzled2 during Xenopus anteroposterior patterning. *Dev. Biol.* **227**, 118-132.

Brunet, J.-P., Tamayo, P., Golub, T. R. and Mesirov, J. P. (2004). Metagenes and molecular pattern discovery using matrix factorization. *Proc. Natl. Acad. Sci. USA* **101**, 4164-4169.

Cao, L., Gibson, J. D., Miyamoto, S., Sail, V., Verma, R., Rosenberg, D. W., Nelson, C. E. and Giardina, C. (2011). Intestinal lineage commitment of embryonic stem cells. *Differentiation* **81**, 1-10.

Cao, L., Kuratnik, A., Xu, W., Gibson, J. D., Kolling, F., Falcone, E. R., Ammar, M., Van Heyst, M. D., Wright, D. L., Nelson, C. E. et al. (2015). Development of intestinal organoids as tissue surrogates: cell composition and the epigenetic control of differentiation. *Mol. Carcinog.* **54**, 189-202.

Chen, Y.-J., Finkbeiner, S. R., Weinblatt, D., Emmett, M. J., Tameire, F., Yousefi, M., Yang, C., Maehr, R., Zhou, Q., Shemer, R. et al. (2014). De novo formationof insulin-producing "'neo-b cell islets'" from intestinal crypts. *Cell Rep.* **6**, 1046-1058.

Cox, W. G. and Hemmati-Brivanlou, A. (1995). Caudalization of neural fate by tissue recombination and bFGF. *Development* **121**, 4349-4358.

Dale, L., Howes, G., Price, B. M. and Smith, J. C. (1992). Bone morphogenetic protein 4: a ventralizing factor in early Xenopus development. *Development* **115**, 573-585.

Dessimoz, J., Opoka, R., Kordich, J. J., Grapin-Botton, A. and Wells, J. M. (2006). FGF signaling is necessary for establishing gut tube domains along the anterior-posterior axis in vivo. *Mech. Dev.* **123**, 42-55.

Domingos, P. M., Itasaki, N., Jones, C. M., Mercurio, S., Sargent, M. G., Smith, J. C. and Krumlauf, R. (2001). The Wnt/beta-catenin pathway posteriorizes neural tissue in Xenopus by an indirect mechanism requiring FGF signalling. *Dev. Biol.* **239**, 148-160.

Duluc, I., Freund, J. N., Leberquier, C. and Kedinger, M. (1994). Fetal endoderm primarily holds the temporal and positional information required for mammalian intestinal development. *J. Cell Biol.* **126**, 211-221.

Duluc, I., Hoff, C., Kedinger, M. and Freund, J.-N. (2001). Differentially expressed endoderm and mesenchyme genes along the fetal rat intestine. *Genesis* **29**, 55-59.

Dusing, M. R., Florence, E. A. and Wiginton, D. A. (2001). Pdx-1 is required for activation in vivo from a duodenum-specific enhancer. *J. Biol. Chem.* **276**, 14434-14442.

Dye, B. R., Hill, D. R., Ferguson, M. A., Tsai, Y.-H., Nagy, M. S., Dyal, R., Wells, J. M., Mayhew, C. N., Nattiv, R., Klein, O. D. et al. (2015). In vitro generation of human pluripotent stem cell derived lung organoids. *eLife* **4**, 05098.

Engevik, M. A., Engevik, K. A., Yacyshyn, M. B., Wang, J., Hassett, D. J., Darien, B., Yacyshyn, B. R. and Worrell, R. T. (2015a). Human Clostridium difficile infection: inhibition of NHE3 and microbiota profile. *Am. J. Physiol. Gastrointest. Liver Physiol.* **308**, G497-G509.

Engevik, M. A., Yacyshyn, M. B., Engevik, K. A., Wang, J., Darien, B., Hassett, D. J., Yacyshyn, B. R. and Worrell, R. T. (2015b). Human Clostridium difficile infection: altered mucus production and composition. *Am. J. Physiol. Gastrointest. Liver Physiol.* **308**, G510-G524.

Erter, C. E., Wilm, T. P., Basler, N., Wright, C. V. and Solnica-Krezel, L. (2001). Wnt8 is required in lateral mesendodermal precursors for neural posteriorization in vivo. *Development* **128**, 3571-3583.

Finkbeiner, S. R., Zeng, X.-L., Utama, B., Atmar, R. L., Shroyer, N. F. and Estes, M. K. (2012). Stem cell-derived human intestinal organoids as an infection model for rotaviruses. *mBio* **3**, e00159-e00112.

Finkbeiner, S. R., Freeman, J. J., Wieck, M. M., El-Nachef, W., Altheim, C. H., Tsai, Y.-H., Huang, S., Dyal, R., White, E. S., Grikscheit, T. C. et al. (2015a). Generation of tissue-engineered small intestine using embryonic stem cell-derived human intestinal organoids. *Biol. Open* **4**, 1462-1472.

Finkbeiner, S. R., Hill, D. R., Altheim, C. H., Dedhia, P. H., Taylor, M. J., Tsai, Y.-H., Chin, A. M., Mahe, M. M., Watson, C. L., Freeman, J. J. et al. (2015b). Transcriptome-wide analysis reveals hallmarks of human intestine development and maturation in vitro and in vivo. *Stem Cell Rep.* **4**, 1140-1155.

Gao, N. and Kaestner, K. H. (2010). Cdx2 regulates endo-lysosomal function and epithelial cell polarity. *Genes Dev.* **24**, 1295-1305.

Gao, N., White, P. and Kaestner, K. H. (2009). Establishment of intestinal identity and epithelial-mesenchymal signaling by Cdx2. *Dev. Cell* **16**, 588-599.

Grainger, S., Savory, J. G. A. and Lohnes, D. (2010). Cdx2 regulates patterning of the intestinal epithelium. *Dev. Biol.* **339**, 155-165.

Greco, T. L., Takada, S., Newhouse, M. M., McMahon, J. A., McMahon, A. P. and Camper, S. A. (1996). Analysis of the vestigial tail mutation demonstrates that Wnt-3a gene dosage regulates mouse axial development. *Genes Dev.* **10**, 313-324.

Gregorieff, A., Grosschedl, R. and Clevers, H. (2004). Hindgut defects and transformation of the gastro-intestinal tract in Tcf4(−/−)/Tcf1(−/−) embryos. *EMBO J.* **23**, 1825-1833.

Hannan, N. R. F., Fordham, R. P., Syed, Y. A., Moignard, V., Berry, A., Bautista, R., Hanley, N. A., Jensen, K. B. and Vallier, L. (2013). Generation of multipotent foregut stem cells from human pluripotent stem cells. *Stem Cell Rep.* **1**, 293-306.

Heijmans, J., de Jeude, J., Koo, B.-K. and Rosekrans, S. L. (2013). ER stress causes rapid loss of intestinal epithelial stemness through activation of the unfolded protein response. *Cell Rep.* **3**, 1128-1139.

Ho, R. K. and Kimmel, C. B. (1993). Commitment of cell fate in the early zebrafish embryo. *Science* **261**, 109-111.

Hollyday, M., McMahon, J. A. and McMahon, A. P. (1995). Wnt expression patterns in chick embryo nervous system. *Mech. Dev.* **52**, 9-25.

Horb, M. E. and Slack, J. M. W. (2001). Endoderm specification and differentiation in Xenopus embryos. *Dev. Biol.* **236**, 330-343.
Howell, J. C. and Wells, J. M. (2011). Generating intestinal tissue from stem cells: potential for research and therapy. *Regen. Med.* **6**, 743-755.
Huelsken, J., Vogel, R., Brinkmann, V., Erdmann, B., Birchmeier, C. and Birchmeier, W. (2000). Requirement for beta-catenin in anterior-posterior axis formation in mice. *J. Cell Biol.* **148**, 567-578.
Ikeya, M. and Takada, S. (2001). Wnt-3a is required for somite specification along the anteroposterior axis of the mouse embryo and for regulation of cdx-1 expression. *Mech. Dev.* **103**, 27-33.
Isaacs, H. V., Pownall, M. E. and Slack, J. M. W. (1998). Regulation of Hox gene expression and posterior development by the Xenopus caudal homologue Xcad3. *EMBO J.* **17**, 3413-3427.
Kedinger, M., Duluc, I., Fritsch, C., Lorentz, O., Plateroti, M. and Freund, J. N. (1998). Intestinal epithelial-mesenchymal cell interactions. *Ann. N. Y. Acad. Sci.* **859**, 1-17.
Keenan, I. D., Sharrard, R. M. and Isaacs, H. V. (2006). FGF signal transduction and the regulation of Cdx gene expression. *Dev. Biol.* **299**, 478-488.
Kiecker, C. and Niehrs, C. (2001). A morphogen gradient of Wnt/beta-catenin signalling regulates anteroposterior neural patterning in Xenopus. *Development* **128**, 4189-4201.
Langmead, B. and Salzberg, S. L. (2012). Fast gapped-read alignment with Bowtie 2. *Nat. Methods* **9**, 357-359.
Lee, D. D. and Seung, H. S. (1999). Learning the parts of objects by non-negative matrix factorization. *Nature* **401**, 788-791.
Lekven, A. C., Thorpe, C. J., Waxman, J. S. and Moon, R. T. (2001). Zebrafish wnt8 encodes two wnt8 proteins on a bicistronic transcript and is required for mesoderm and neurectoderm patterning. *Dev. Cell* **1**, 103-114.
Leslie, J. L., Huang, S., Opp, J. S., Nagy, M. S., Kobayashi, M., Young, V. B. and Spence, J. R. (2014). Persistence and toxin production by Clostridium difficile within human intestinal organoids results in disruption of epithelial paracellular barrier function. *Infect. Immun.* **83**, 138-145.
Levin, D. E., Barthel, E. R., Speer, A. L., Sala, F. G., Hou, X., Torashima, Y. and Grikscheit, T. C. (2013). Human tissue-engineered small intestine forms from postnatal progenitor cells. *J. Pediatr. Surg.* **48**, 129-137.
Lickert, H., Domon, C., Huls, G., Wehrle, C., Duluc, I., CLEVERS, H., Meyer, B. I., Freund, J. N. and Kemler, R. (2000). Wnt/(beta)-catenin signaling regulates the expression of the homeobox gene Cdx1 in embryonic intestine. *Development* **127**, 3805-3813.
Liu, P., Wakamiya, M., Shea, M. J., Albrecht, U., Behringer, R. R. and Bradley, A. (1999). Requirement for Wnt3 in vertebrate axis formation. *Nat. Genet.* **22**, 361-365.
Marvin, M. J., Di Rocco, G., Gardiner, A., Bush, S. M. and Lassar, A. B. (2001). Inhibition of Wnt activity induces heart formation from posterior mesoderm. *Genes Dev.* **15**, 316-327.
McCracken, K. W., Howell, J. C., Spence, J. R. and Wells, J. M. (2011). Generating human intestinal tissue from pluripotent stem cells in vitro. *Nat. Protoc.* **6**, 1920-1928.
McLin, V. A., Rankin, S. A. and Zorn, A. M. (2007). Repression of Wnt/(beta)-catenin signaling in the anterior endoderm is essential for liver and pancreas development. *Development* **134**, 2207-2217.
Middendorp, S., Schneeberger, K., Wiegerinck, C. L., Mokry, M., Akkerman, R. D. L., van Wijngaarden, S., Clevers, H. and Nieuwenhuis, E. E. S. (2014). Adult stem cells in the small intestine are intrinsically programmed with their location-specific function. *Stem Cells* **32**, 1083-1091.
Mootha, V. K., Lindgren, C. M., Eriksson, K.-F., Subramanian, A., Sihag, S., Lehar, J., Puigserver, P., Carlsson, E., Ridderstråle, M., Laurila, E. et al. (2003). PGC-1alpha-responsive genes involved in oxidative phosphorylation are coordinately downregulated in human diabetes. *Nat. Genet.* **34**, 267-273.
Northrop, J. L. and Kimelman, D. (1994). Dorsal-ventral differences in Xcad-3 expression in response to FGF-mediated induction in Xenopus. *Dev. Biol.* **161**, 490-503.
Parr, B. A. and McMahon, A. P. (1995). Dorsalizing signal Wnt-7a required for normal polarity of D-V and A-P axes of mouse limb. *Nature* **374**, 350-353.
Pownall, M. E., Tucker, A. S., Slack, J. M. and Isaacs, H. V. (1996). eFGF, Xcad3 and Hox genes form a molecular pathway that establishes the anteroposterior axis in Xenopus. *Development* **122**, 3881-3892.
Ratineau, C., Duluc, I., Pourreyron, C., Kedinger, M., Freund, J.-N. and Roche, C. (2003). Endoderm- and mesenchyme-dependent commitment of the differentiated epithelial cell types in the developing intestine of rat. *Differentiation* **71**, 163-169.
Rockich, B. E., Hrycaj, S. M., Shih, H.-P., Nagy, M. S., Ferguson, M. A. H., Kopp, J. L., Sander, M., Wellik, D. M. and Spence, J. R. (2013). Sox9 plays multiple roles in the lung epithelium during branching morphogenesis. *Proc. Natl. Acad. Sci. USA* **110**, E4456-E4465.
Rodansky, E. S., Johnson, L. A., Huang, S., Spence, J. R. and Higgins, P. D. R. (2015). Intestinal organoids: a model of intestinal fibrosis for evaluating anti-fibrotic drugs. *Exp. Mol. Pathol.* **98**, 345-351.
Rothenberg, M. E., Nusse, Y., Kalisky, T., Lee, J. J., Dalerba, P., Scheeren, F., Lobo, N., Kulkarni, S., Sim, S., Qian, D. et al. (2012). Identification of a cKit+ colonic crypt base secretory cell that supports lgr5+ stem cells in mice. *Gastroenterology* **142**, 1195-1205.e6.
Satoh, W., Gotoh, T., Tsunematsu, Y., Aizawa, S. and Shimono, A. (2006). Sfrp1 and Sfrp2 regulate anteroposterior axis elongation and somite segmentation during mouse embryogenesis. *Development* **133**, 989-999.
Sherwood, R. I., Chen, T.-Y. A. and Melton, D. A. (2009). Transcriptional dynamics of endodermal organ formation. *Dev. Dyn.* **238**, 29-42.
Sherwood, R. I., Maehr, R., Mazzoni, E. O. and Melton, D. A. (2011). Wnt signaling specifies and patterns intestinal endoderm. *Mech. Dev.* **128**, 14.
Spence, J. R., Mayhew, C. N., Rankin, S. A., Kuhar, M. F., Vallance, J. E., Tolle, K., Hoskins, E. E., Kalinichenko, V. V., Wells, S. I., Zorn, A. M. et al. (2011). Directed differentiation of human pluripotent stem cells into intestinal tissue in vitro. *Nature* **470**, 105-109.
Subramanian, A., Tamayo, P., Mootha, V. K., Mukherjee, S., Ebert, B. L., Gillette, M. A., Paulovich, A., Pomeroy, S. L., Golub, T. R., Lander, E. S. et al. (2005). Gene set enrichment analysis: a knowledge-based approach for interpreting genome-wide expression profiles. *Proc. Natl. Acad. Sci. USA* **102**, 15545-15550.
Tamminen, K., Balboa, D., Toivonen, S., Pakarinen, M. P., Wiener, Z., Alitalo, K. and Otonkoski, T. (2015). Intestinal commitment and maturation of human pluripotent stem cells is independent of exogenous FGF4 and R-spondin1. *PLoS ONE* **10**, e0134551.
Uhlén, M., Oksvold, P., Fagerberg, L., Lundberg, E., Jonasson, K., Forsberg, M., Zwahlen, M., Kampf, C., Wester, K., Hober, S. et al. (2010). Towards a knowledge-based Human Protein Atlas. *Nat. Biotechnol.* **28**, 1248-1250.
Ullrich, T., Tang, Y.-W., Correa, H., Garzon, S. A., Maheshwari, A., Hill, M., Matta, P., Krishnan, M. K. and Weitkamp, J.-H. (2012). Absence of gastrointestinal pathogens in ileum tissue resected for necrotizing enterocolitis. *Pediatr. Infect. Dis. J.* **31**, 413-414.
Verzi, M. P., Shin, H., He, H. H., Sulahian, R., Meyer, C. A., Montgomery, R. K., Fleet, J. C., Brown, M., Liu, X. S. and Shivdasani, R. A. (2010). Differentiation-specific histone modifications reveal dynamic chromatin interactions and partners for the intestinal transcription factor CDX2. *Dev. Cell* **19**, 713-726.
Verzi, M. P., Shin, H., San Roman, A. K., Liu, X. S. and Shivdasani, R. A. (2013). Intestinal master transcription factor CDX2 controls chromatin access for partner transcription factor binding. *Mol. Cell. Biol.* **33**, 281-292.
Wang, X., Yamamoto, Y., Wilson, L. H., Zhang, T., Howitt, B. E., Farrow, M. A., Kern, F., Ning, G., Hong, Y., Khor, C. C. et al. (2015). Cloning and variation of ground state intestinal stem cells. *Nature* **522**, 173-178.
Watson, C. L., Mahe, M. M., Múnera, J., Howell, J. C., Sundaram, N., Poling, H. M., Schweitzer, J. I., Vallance, J. E., Mayhew, C. N., Sun, Y. et al. (2014). An in vivo model of human small intestine using pluripotent stem cells. *Nat. Med.* **20**, 1310-1314.
Wells, J. M. and Melton, D. A. (1999). Vertebrate endoderm development. *Annu. Rev. Cell Dev. Biol.* **15**, 393-410.
Wells, J. M. and Melton, D. A. (2000). Early mouse endoderm is patterned by soluble factors from adjacent germ layers. *Development* **127**, 1563-1572.
Xue, X., Ramakrishnan, S., Anderson, E., Taylor, M., Zimmermann, E. M., Spence, J. R., Huang, S., Greenson, J. K. and Shah, Y. M. (2013). Endothelial PAS domain protein 1 activates the inflammatory response in the intestinal epithelium to promote colitis in mice. *Gastroenterology* **145**, 831-841.
Zorn, A. M. and Wells, J. M. (2007). Molecular basis of vertebrate endoderm development. *Int. Rev. Cytol.* **259**, 49-111.

Supplemental Information

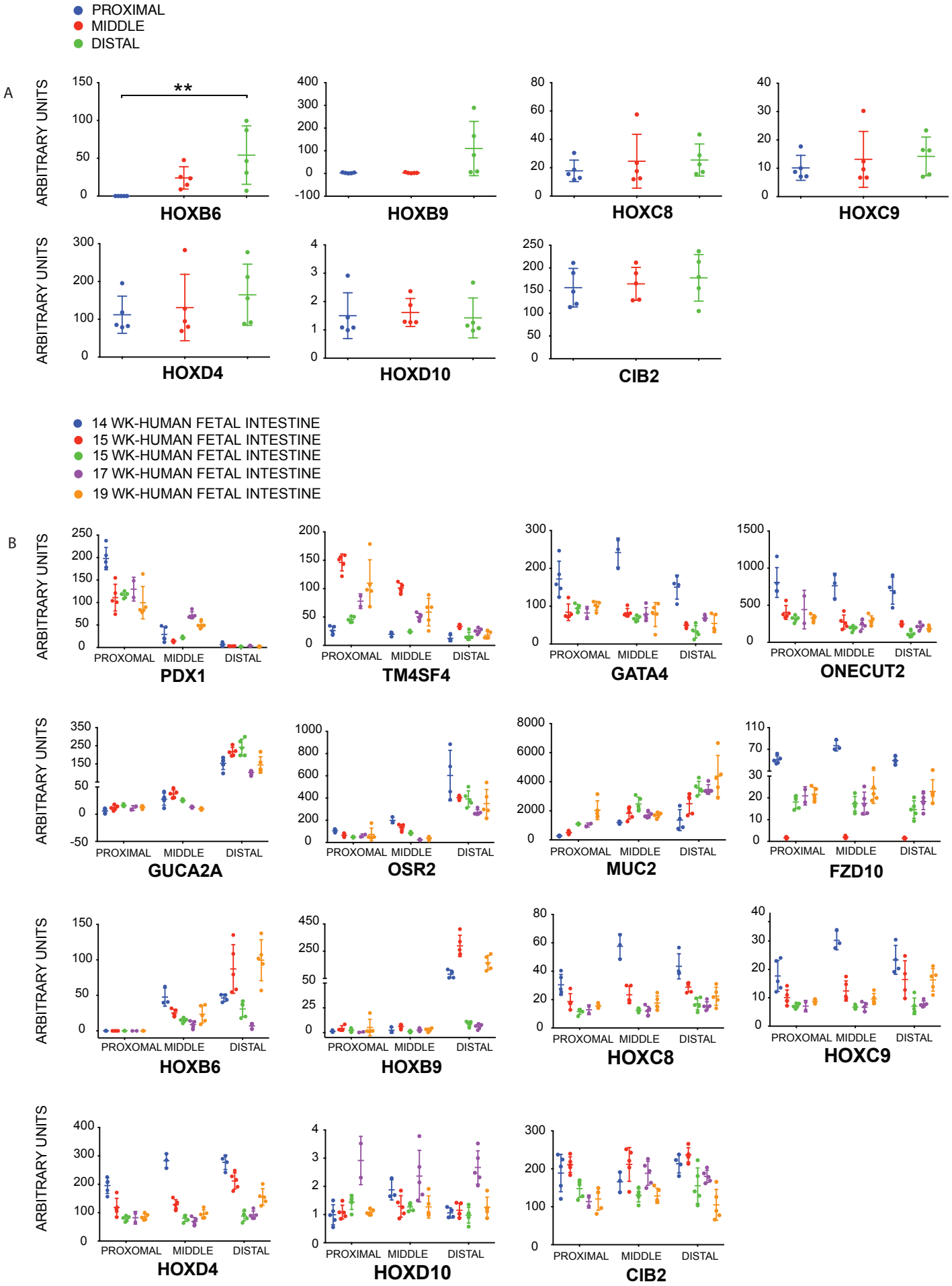

Supplemental Figure 1, Related to Figure 1
A) Genes demonstrated to be regionally expressed in mice, including several HOX genes, were examined in different regions of the human fetal small intestine (n= 5 individual samples; proximal – blue, middle – red, distal – green). Only *HOXB5* was regionally expressed, with highest expression in the distal small intestine.
B) Individual biological specimens (n=5) of the human fetal small intestine examined in Figure 1 and Supplemental Figure 1A were plotted for their gene expression in the proximal, middle or distal region. Each color corresponds to an individual sample (blue - 14 week; red – 15 week; green – 15 week; purple – 17 week; orange – 19 week), and each data point for an individual samples is a technical replicate.

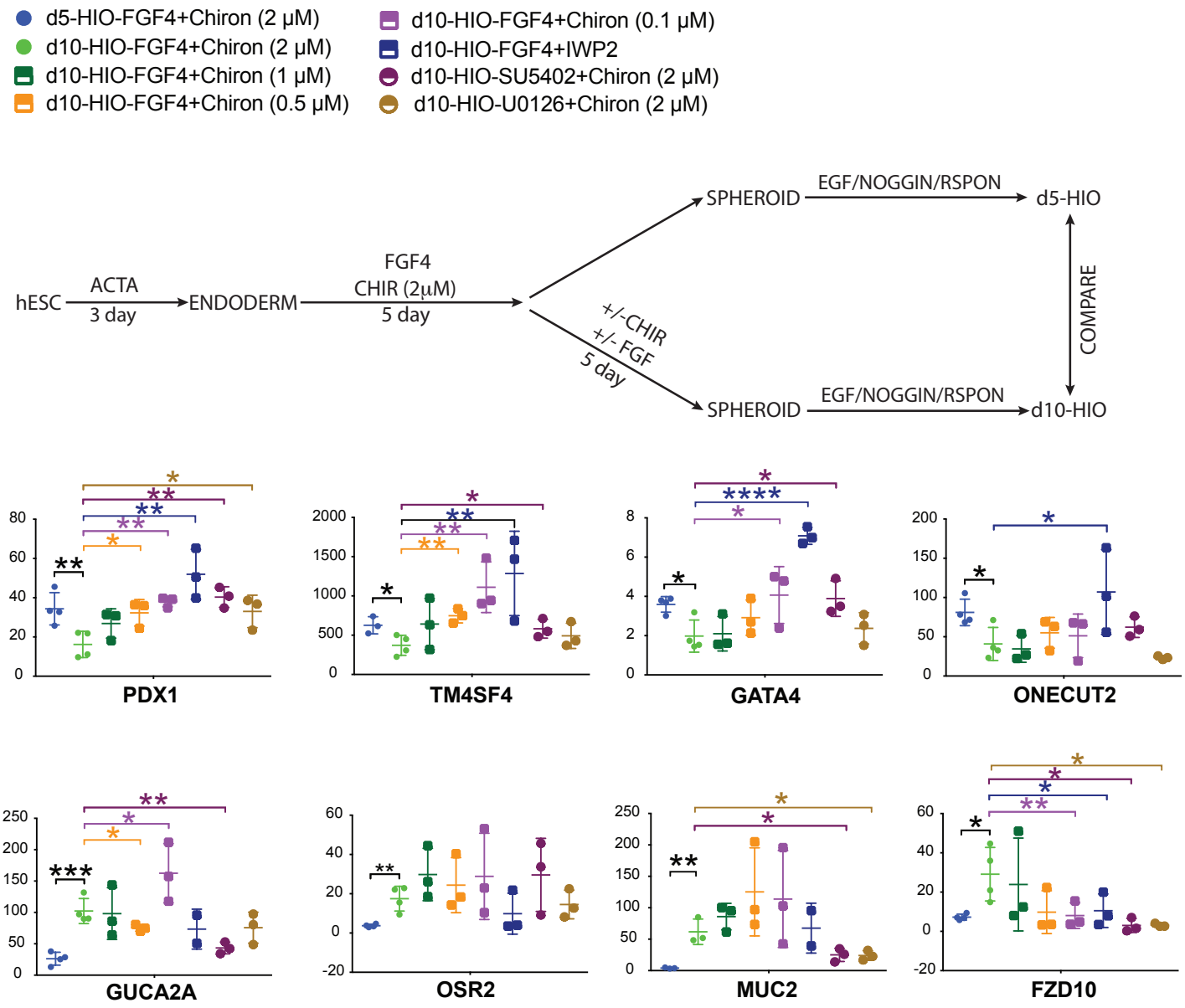

Supplemental Figure 2, related to Figure 2
Top) Schematic of the experimental design, indicating that endoderm was treated for 5 days with FGF4/CHIR99021, and seeded in matrigel for expansion into organoids (top branch of schematic). For the next 5 days, cultures were treated with varying concentrations of CHIR99021 (see legend at top), or in inhibitors of WNT-signaling (IWP2), FGF signaling (SU5402) or the ERK inhibitor (UO126) (bottom branch of schematic). Spheroids from different conditions were seeded into matrigel and expanded into organoids.
Bottom) Genes examined in the different conditions, included the proximal small intestinal markers *PDX1, TM4SF4, GATA4, ONECUT2* or the distal small intestinal markers *GUCA2A, OSR2, MUC2, FZD10.*

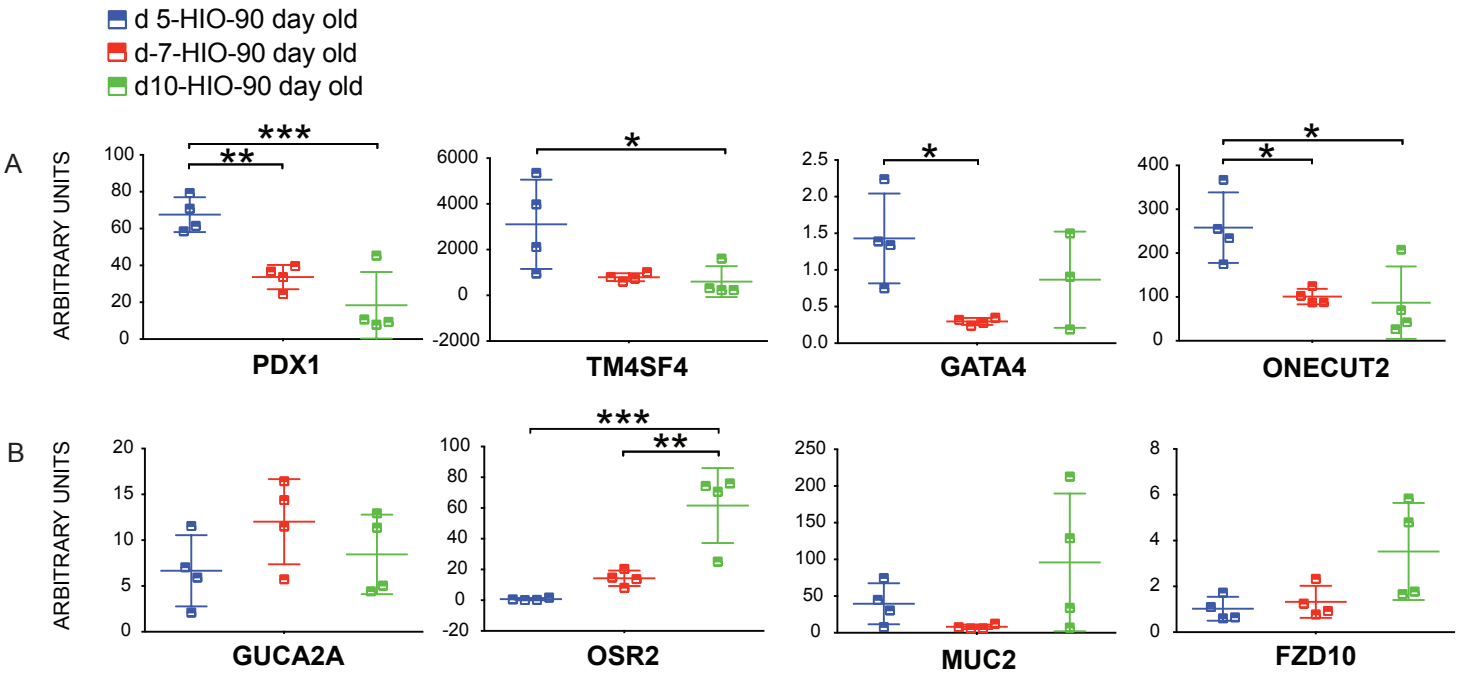

Supplemental Figure 3, related to Figure 2
Regionally expressed genes were examined in d5, d7 and d10 organoids after 90 days of *in vitro* growth. Genes examined in 90 day organoids included the proximal small intestinal markers *PDX1, TM4SF4, GATA4, ONECUT2* or the distal small intestinal markers *GUCA2A, OSR2, MUC2, FZD10.*

Supplemental Figure 4

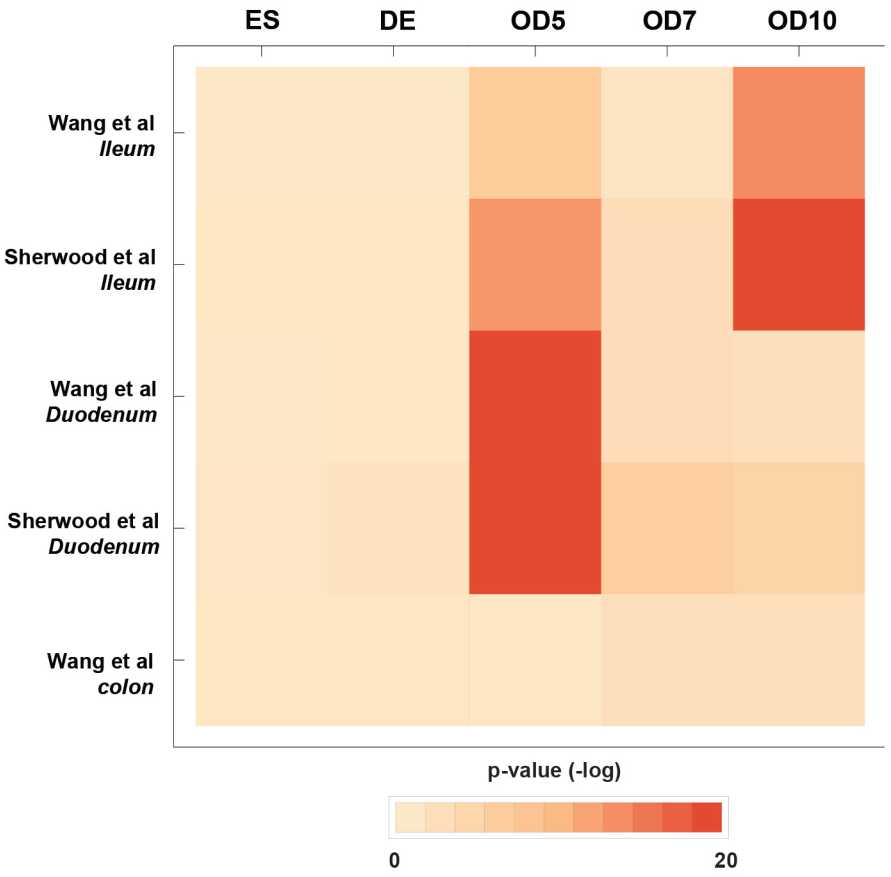

Supplemental Figure 4, related to Figure 3
Enriched genes in d5, d7 and d10 organoids were compared to published gene lists of that are regionally restricted to the duodenum or the ileum and colon. A hypergeometric test was used to determine the level of significance of overlapping gene sets. Gene overlap between d5, d7 and d10 data sets with colonic tissue in not statistically significant.

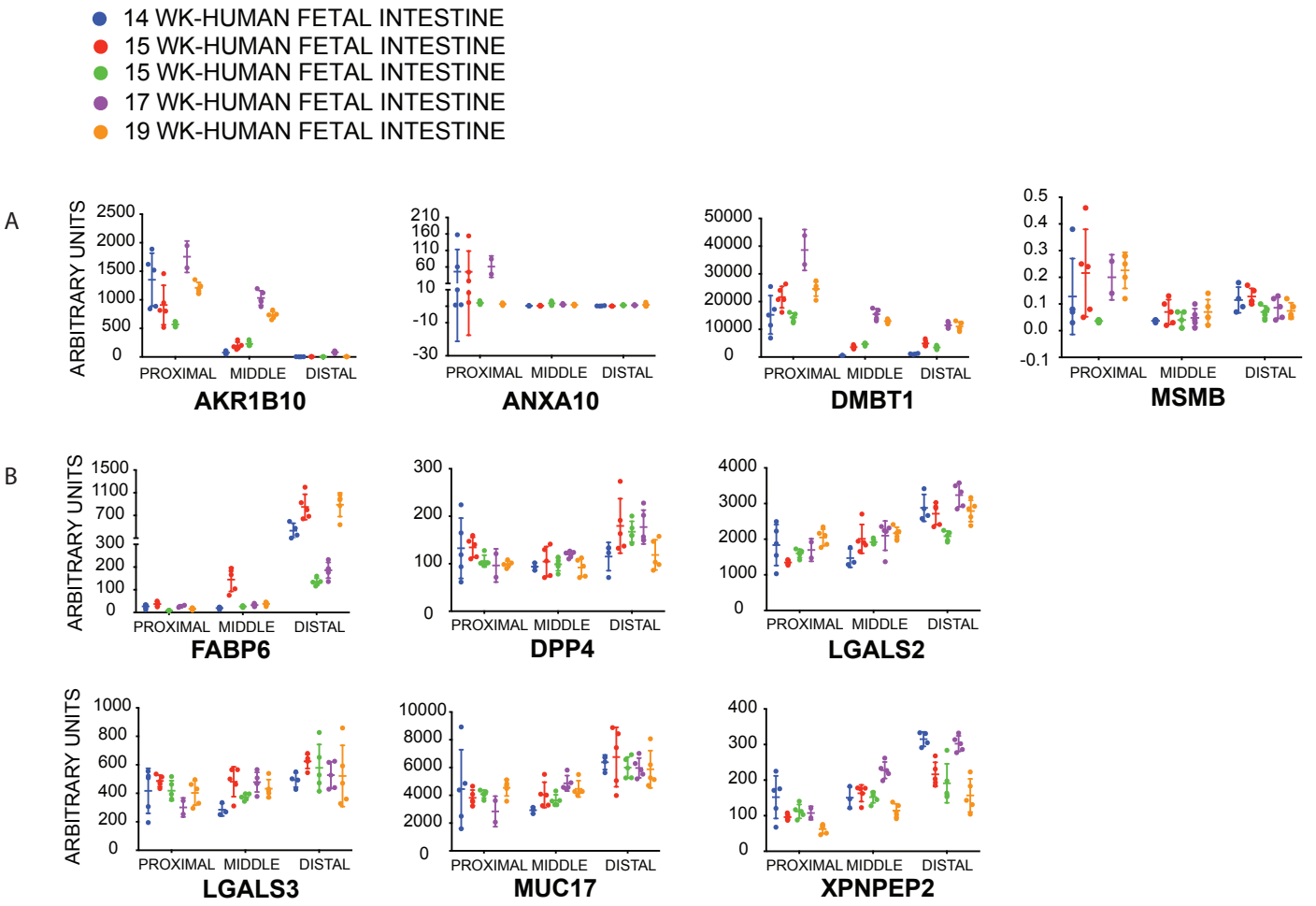

Supplemental Figure 5, related to Figure 4
Individual biological speciments (n=5) of the human fetal small intestine examined in Figure 4 were plotted for their gene expression in the proximal, middle or distal region. Each color corresponds to an individual sample (blue - 14 week; red – 15 week; green – 15 week; purple – 17 week; orange – 19 week), and each data point for an individual samples is a technical replicate.

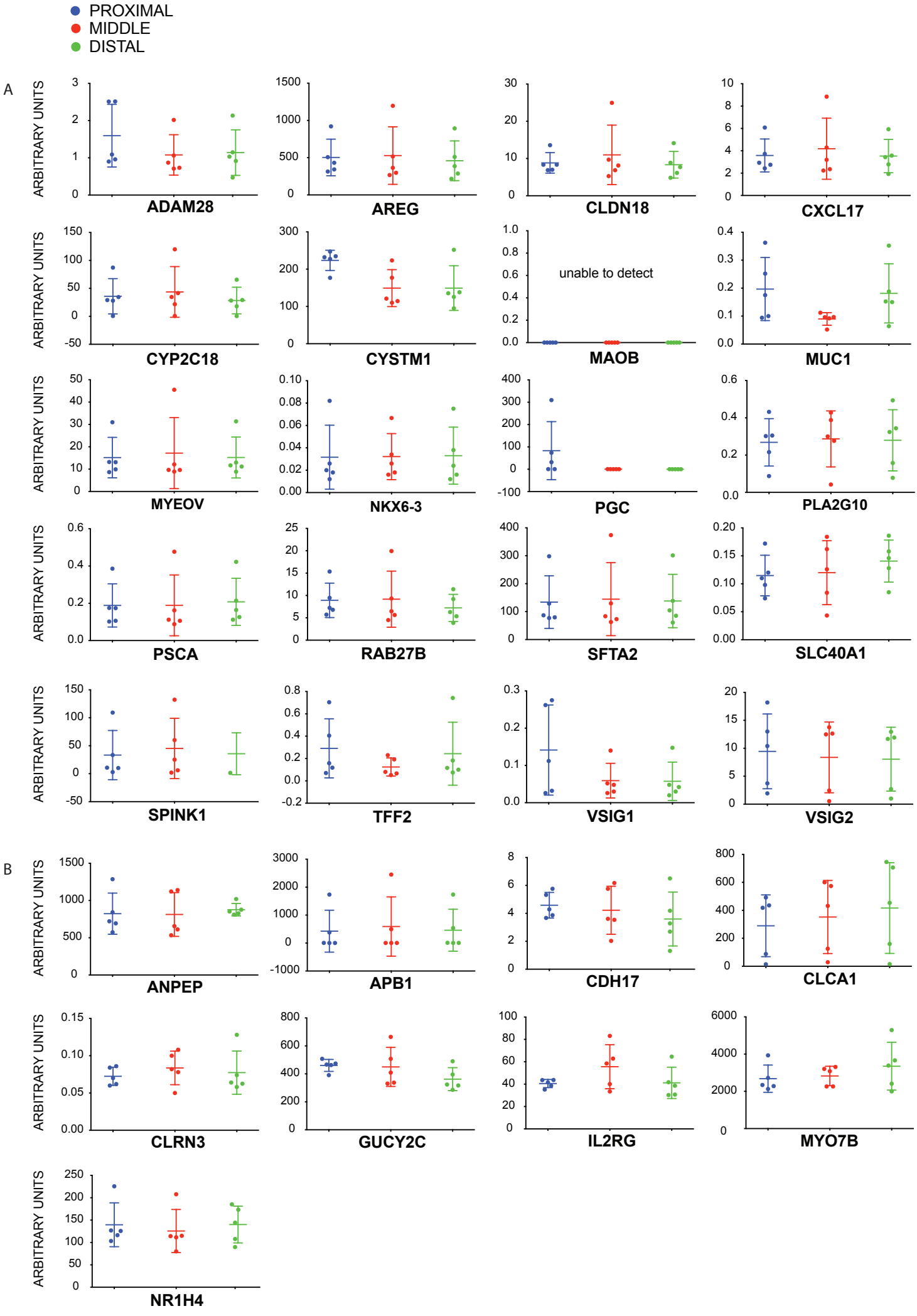

Supplemental Figure 6, related to Figure 3
A) Genes identified as overlapping between d5 organoids and duodenal genes Figure 3B and Figure 3C that did not show corresponding proximal enrichment in human fetal intestine (n=5 independent biological samples; proximal – blue, middle – red, distal – green).

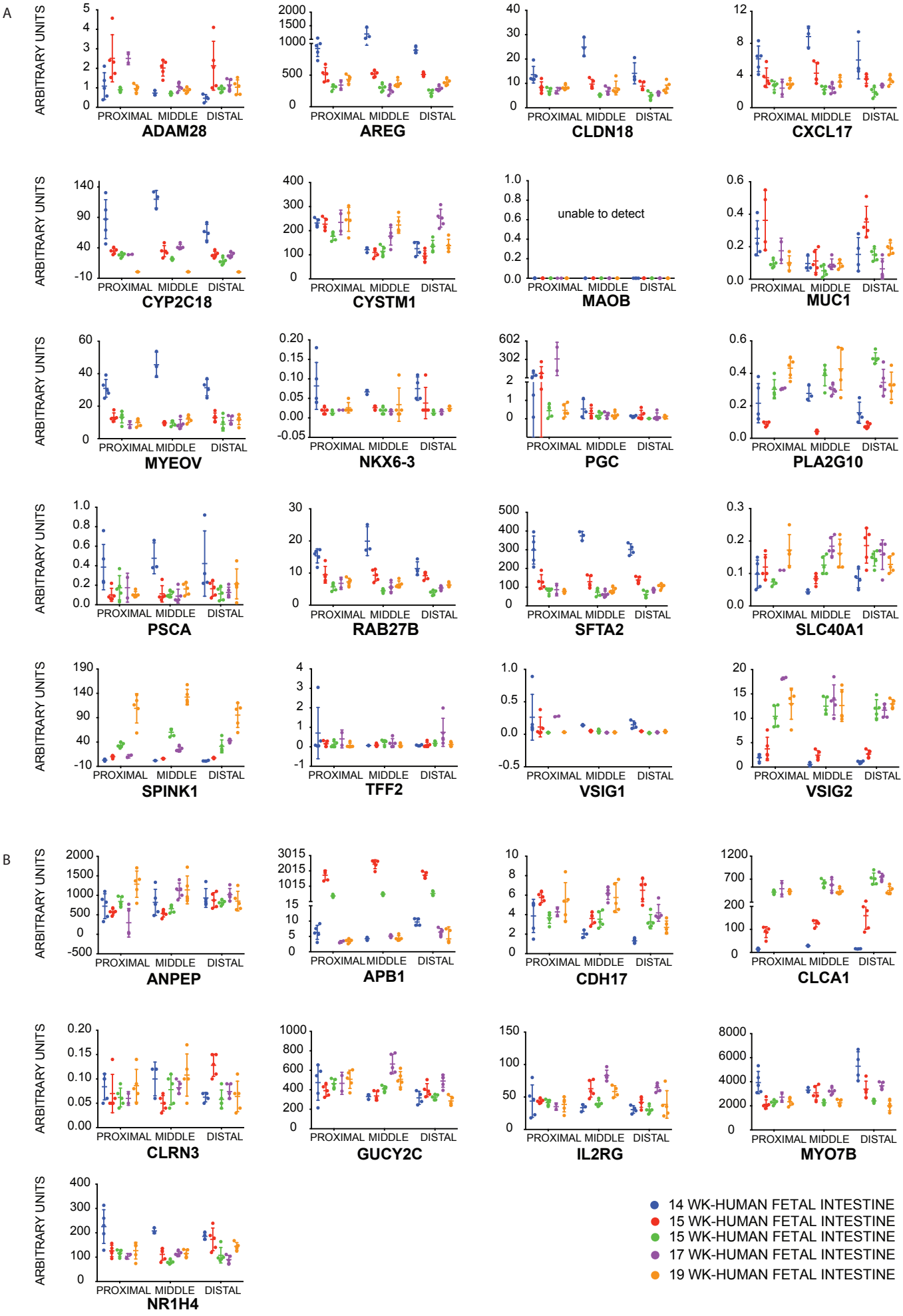

Supplemental Figure 7, related to Figure 3 and Supplemental Figure 6
Individual biological speciments (n=5) of the human fetal small intestine examined in Supplemental Figure 6 were plotted for their gene expression in the proximal, middle or distal region. Each color corresponds to an individual sample (blue - 14 week; red – 15 week; green – 15 week; purple – 17 week; orange – 19 week), and each data point for an individual samples is a technical replicate.

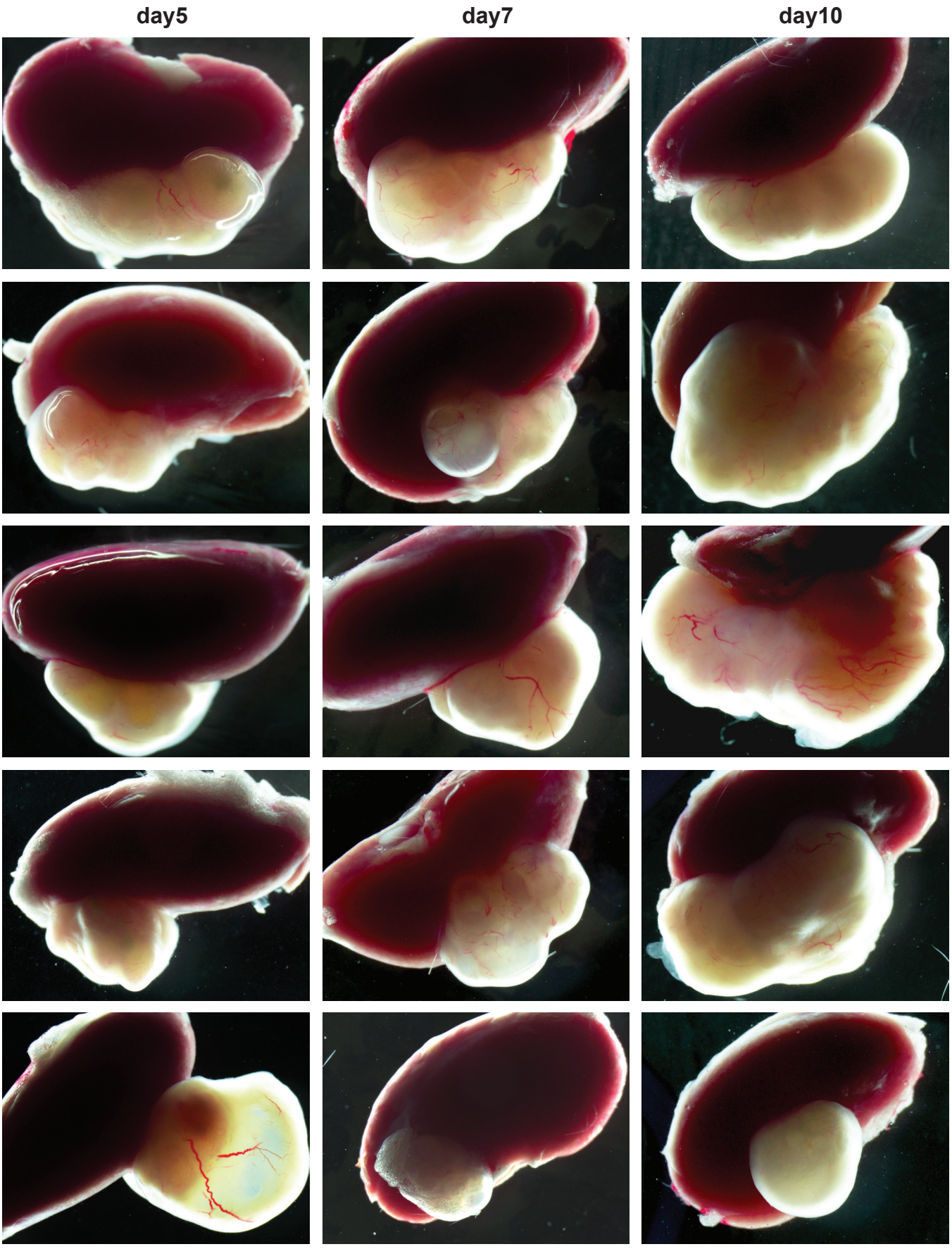

Supplemental Figure 8, Related to Figure 5
d5, d7 and d10 organoids were transplanted under the kidney capsule, and were harvested after 10 weeks. 5 independent transplants for each group of organoids are shown.

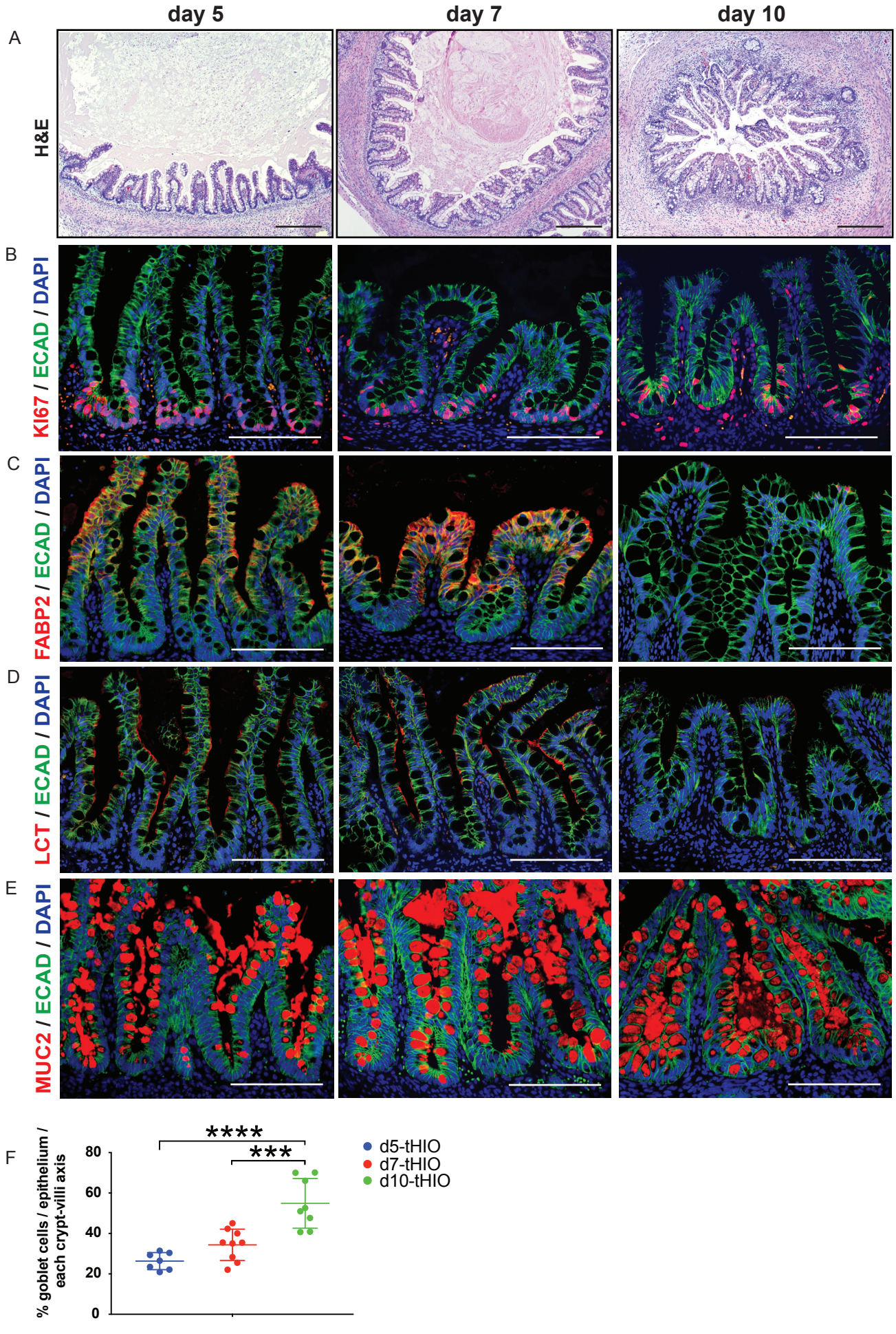

Supplemental Figure 9, Related to Figure 5

A) Low magnification H&E staining of transplanted d5, d7 and d10 organoids after 10 weeks.

B) d5, d7 and d10 transplanted organoids were stained for ECAD (green), the proliferation marker, KI67 (red) and nuclei (DAPI, blue). Note that epithelial proliferation is restricted to the base of the epithelium.

C) d5, d7 and d10 transplanted organoids were stained for ECAD (green), FABP2 (red) and nuclei (DAPI, blue). FABP2 is normally expressed in the proximal intestine, and shows expression in only the d5 and d7 transplanted organoids.

D) d5, d7 and d10 transplanted organoids were stained for ECAD (green), Lactase (LCT, red) and nuclei (DAPI, blue). LCT is normally expressed in the proximal intestine, and shows expression in only the d5 and d7 transplanted organoids.

E) d5, d7 and d10 transplanted organoids were stained for ECAD (green), MUC2 (red) and nuclei (DAPI, blue). MUC2 is normally expressed in goblet cells throughout the small intestine, which are more abundant in the distal intestine (ileum).

F) MUC2+ Goblet cells were quantitated from sections of d5 (n=7 individual transplants), d7 (n=9 individual transplants) or d10 (n=8 individual transplants) organoids.

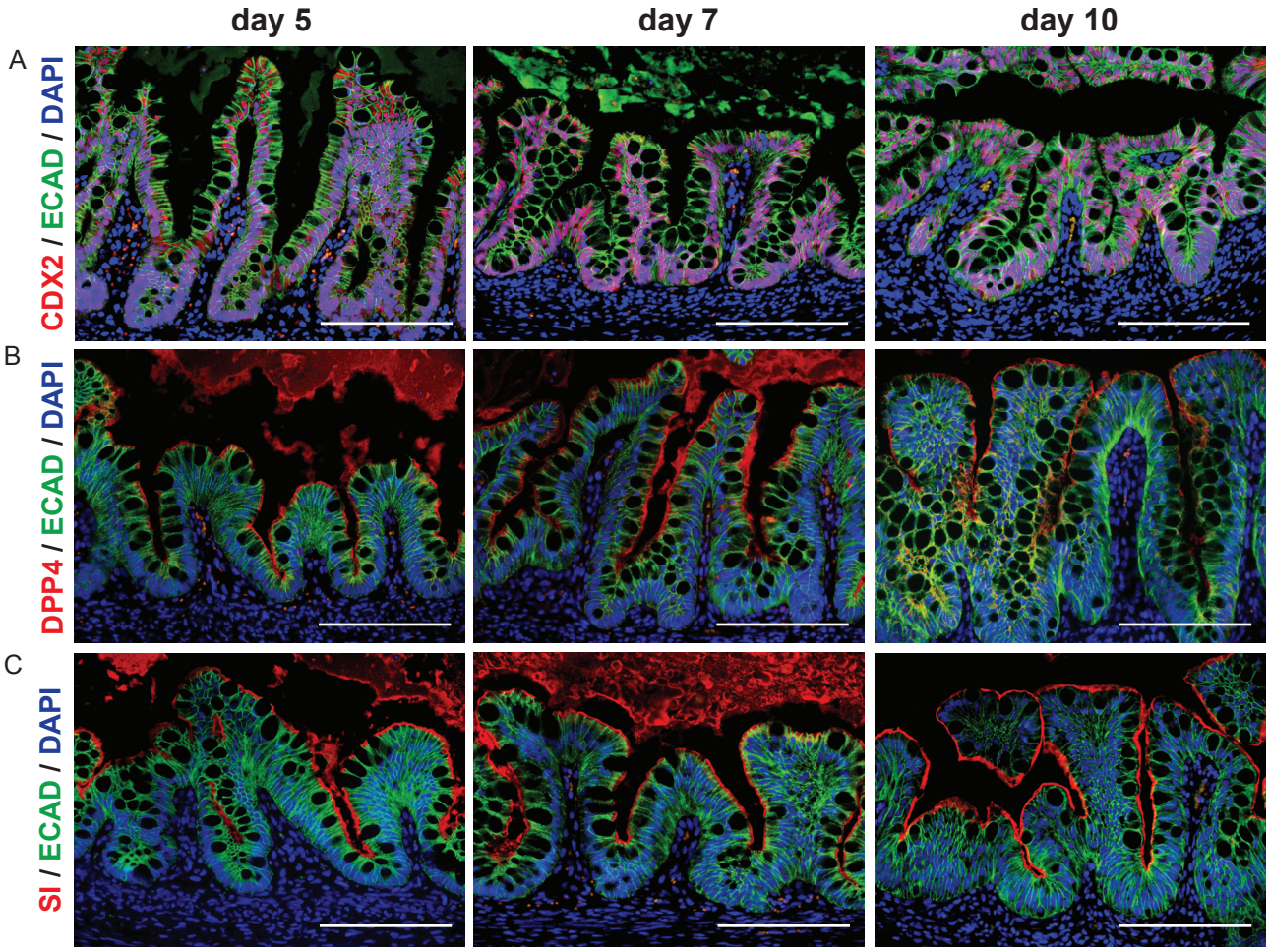

Supplemental Figure 10, Related to Figure 5
A) d5, d7 and d10 transplanted organoids were stained for ECAD (green), the intestinal marker, CDX2 (red) and nuclei (DAPI, blue).
B) d5, d7 and d10 transplanted organoids were stained for ECAD (green), DPPIV (red) and nuclei (DAPI, blue). DPPIV is normally expressed in enterocytes throughout the small intestine, and showed expression in all organoid groups examined.
C) d5, d7 and d10 transplanted organoids were stained for ECAD (green), Sucrase Isomaltase (SI, red) and nuclei (DAPI, blue). DPPIV is normally expressed in enterocytes throughout the small intestine, and showed expression in all organoid groups examined.

Table S1. Stage-specific gene expression programs

ES	DE	ORG 5	ORG 7	ORG 10
LEUTX	OR6B1	CSHL1	OR2M3	CT47A10
DUX2	CRLF2	CA6	XAGE2B	OR3A3
CUZD1	CT47A1	NKX6-3	CT47A4	CSHL1
SEMG1	CD48	GC	DUSP21	PRAMEF20
DPEP3	DEFB106A	GKN1	KRTAP19-7	LCN15
IDO1	RLN3	DEFB116	GAGE12D	SLC17A4
AHSP	NCR1	BSX	DEFB103B	KRTAP13-3
HHLA1	ACSM4	PRAMEF21	S100A9	NXPE1
HIST1H2BA	GSC	PI3	KRT4	GAGE12F
DAZL	LCE5A	HABP2	KRT5	GAGE8
PLA2G4C	RFPL2	MYBPC1	MUC16	C17orf78
SCGB3A2	LGALS12	COMP	KRT13	PNCK
KRTAP8-1	CHAT	GKN2	KRT6A	DEFA5
P2RX5	OR51L1	ADH1C	HCAR2	TMIGD1
UMOD	OR5M1	TFF1	ZBED2	GUCA2A
TRIML2	CER1	PSCA	PADI1	CLDN14
ASIC5	LEFTY1	UBD	GFAP	CCL23
LECT1	CTSF	PGC	CRISP3	LGALS14
GAGE2B	PKHD1L1	TFF2	LCE1F	FCAMR
UCMA	BRDT	MMP3	GDF10	CHGA
TNFSF11	BPY2B	OLFM4	MUC5B	OR4M2
MT1H	FAM135B	IBSP	RANBP3L	CTAG2
ECE2	LEFTY2	UGT1A6	TNNT3	KCNK16
TCL1B	NODAL	AADAC	CRISP2	AOAH
MT1P2	APOBEC3G	MSMB	FTHL17	SLC51A
HPDL	IGFL1	SERPINA1	CLPS	RNF186
MT1G	TMEM150C	MMP7	SCGB2A1	MYO7B
PTGER1	MIXL1	ALB	KRT17	PRAMEF7
CR2	FGF17	IL1R2	C1orf158	TIMD4
RASGRP2	ASB5	SERPINA3	MGP	TNNI2
GPR176	RFPL4A	UGT2B17	AGTR1	EVPL
GH1	OR10H5	CTSE	SCG2	CCL24
FAM46B	ELOVL2	TCN1	CT47A8	CEACAM20
IGSF21	EOMES	VSIG2	PTGDS	CDHR5
ZDHHC22	PGLYRP3	DEFB4A	C20orf85	PRSS41
PROKR2	ARHGAP40	LCN2	FMO3	GPA33
SERPINB4	SERPINB9	VNN2	ANXA8	CHGB
TEX14	CALB1	KRT6B	SPRR1B	FAM5C
HPCAL4	HRASLS5	PIK3C2G	ADAD1	TPH1
KCNK7	GPR151	GPR110	S100A2	KRTAP6-3
OLFM1	OR2B11	CLDN18	AQP5	OR52M1

EMX1	PLSCR2	ITIH2	SLC6A13	TNFRSF14
IL17C	PLXNA4	KRTAP1-1	DMBT1	VMO1
SIT1	IL1RL1	SPP1	GJB6	HAVCR1
CPNE9	MAGEA6	UGT1A7	KLHL41	MAGIX
FAM71F1	OR5P2	FER1L6	MSLN	HMGCS2
KLK5	SLC5A4	ACE2	C7	SLC39A5
C1orf94	WT1	OTOP3	P4HA3	PDZD3
KLHDC7A	JAKMIP1	UGT1A1	COL11A2	LGALS2
DOCK2	CNGA4	UGT1A9	GDF15	SST
PRM1	FOXI1	SLC2A2	ASPN	ANO9
KLK13	OR6C4	SPRR3	SFRP4	MTMR11
PXDNL	SLC35F3	SPINK1	C6orf15	GCG
ERVMER34-1	XAGE1B	SAA1	LCN1	KLK12
SPATA31C2	ANKS1B	DEFB4B	OR2T5	HEPACAM2
MEDAG	TRDN	AMBP	CT47A7	GPR35
RYR1	APOL3	KCNJ16	AQP1	C10orf99
BCL2L10	CYP26A1	TREM1	SERPINB7	OR51E1
PPP2R2B	MEPE	BPIFB1	EMR1	CEACAM18
POLR3G	SYT10	PRSS3	APOD	GUCY2C
TNFRSF8	TDRD7	IL1RN	DCSTAMP	APOC3
MB21D1	SEMA3E	LYZ	DCN	GABRE
ACOXL	ACCSL	UGT2B15	C4A	ASCL2
RIT2	PTPN20A	REG3A	FOSB	CAPN3
IZUMO2	OR10A3	RAET1E	SCEL	NR1I2
CAMKV	TGIF2LX	TM4SF4	C4B_2	FABP4
ATP1A3	IFLTD1	CYP2C18	CT47A11	ANPEP
DEFB103A	GREM2	HPGD	C4B	MUC17
PRKCB	PRSS35	APOL1	PRR21	SYT8
MAS1	FZD8	PDZK1IP1	SLC26A9	LGALS7B
SYN3	CALCR	FDCSP	VGLL1	TTR
FAM25B	MANEA	PRSS2	CILP	MUC2
BCAN	PLXNA2	UGT1A4	AQP3	AIFM3
CRYGD	PPP1R16B	RAB27B	TRIM29	RETNLB
n	GATA6	ADH1A	OGN	PTPN20A
ASB2	SPRR2D	SULT1B1	SLC6A12	MYO1A
POU5F1	TSPY3	KYNU	TBX18	PTCRA
AASS	PIK3R5	UGT2A3	FOS	LGALS4
LPL	EYA2	MMP1	XCR1	FABP1
MS4A15	CTAG1A	CRISP2	HCAR3	ZMYND15
FXYD7	SLC34A2	MUC1	CALML3	S1PR4
IL34	TEX28	LGALS9	CYP2E1	OR52K1
KRTAP27-1	PAGE5	SFTA2	TEKT1	AATK
VSNL1	HHATL	UGT1A8	LAMA2	CNR2

ZSCAN10	SLCO1C1	SCGN	ANXA8L2	DDC
SNTG2	FZD5	MMP12	TNFRSF18	ABCC3
SYT6	CYP3A43	ANXA10	MUC4	TINAG
POU5F1B	OR4D1	IL8	WDR38	SLC6A7
RIMS4	OR6B2	UGT1A5	CA9	NDRG1
ASMT	KRTAP19-1	NRAP	DEFB123	SLC17A1
CYP2A13	KCNF1	ROS1	CFI	CCL14
NT5C1A	CMTM1	C15orf48	SERPINB5	WNK4
LCK	FMN2	MMP13	CASP1	DPT
PRELP	STK31	GBA3	INSRR	SPATA19
ALPPL2	OTX2	CASP5	AGT	CDHR2
HTR2C	HHEX	OR1N1	IGFL2	MLXIPL
THY1	SLITRK2	AKR1B10	ROPN1L	ENTPD8
MYH2	C17orf112	VSIG1	AKR1C1	MOGAT2
CAMK2N2	PDZRN4	REG4	ITGA10	FXYD3
PF4V1	OR6S1	SPINK6	IGFBP5	ABP1
KRTAP11-1	COL5A2	MAOB	KRT6C	PDHA2
SLC38A4	IQCF2	CXCL17	IFI44	GP1BB
CCL26	FAM167A	UGT1A10	POSTN	TMEM150B
USP44	PPAPDC1A	ODAM	GNA15	PCSK1
RTBDN	OR10H1	SLPI	SLPI	OR52K2
HTR7	OR6M1	BTNL8	RARRES3	XPNPEP2
GYLTL1B	FAM159B	ONECUT2	SYNPR	SLCO2B1
C6orf99	GPR33	C3	PI15	OR5J2
CA6	CST6	ITGB6	TGM2	FABP6
C12orf56	TRPA1	FGL1	AKR1C2	OR2T35
ZFP57	SCGB1D2	CFH	LY6D	EPS8L3
HS3ST2	FAM20A	PRSS1	FAM3D	DUX4L2
HES3	PRAMEF5	DUX4L6	LCE3A	DOK7
TNNT2	DUSP13	CLDN2	MMP10	KCNN4
TMEM132B	RHAG	LTB	DENND2D	OR52R1
LHX4	POU2AF1	C4BPB	GAGE12J	AMN
KLF1	FAM24B	SLC4A4	C10orf10	RAET1E
TNNC2	DACT2	CASR	ODAM	KRTAP20-1
GRID2	MT3	ORM1	ABCA8	MAG
FOXD3	OR2M2	MMP9	NKX6-1	CLCA1
KLK8	GAL	SERPINB2	LUM	NXPE2
TAC1	ADAM19	GCKR	SERPINA5	IGFN1
MEIOB	USP2	GPR128	PALMD	GAST
PRR20E	SOX17	CFTR	LCNL1	IL37
KCNK17	B3GNT2	ALDOB	COL1A2	AQP12B
PYDC1	GATA4	MAGEA2	TACSTD2	KIF12
DCAF12L1	TEX101	OAS1	DYNLRB2	MEP1A

VAV1	ABCG4	CCL20	COL3A1	HKDC1
CST11	OR2T4	SAA2	VNN2	APOBEC1
ACSBG1	MAGEA8	CLIC3	KRTAP17-1	LOC646498
KLKB1	BATF3	FCGBP	SPARCL1	BAIAP2L2
TERF1	STC1	CYP1A1	CXCL1	TRABD2A
HHLA3	PHOSPHO1	GIF	FNDC1	CAPN8
SYT3	SLC25A48	GSTA5	FIBIN	PTPRR
NPTX1	SPRR2A	IL15RA	KLK6	GZMM
CABP1	SSUH2	AKR1C4	PRAMEF21	PRSS58
SNCB	KCNK12	AREG	C4BPA	AMICA1
SPRR2F	PITX2	UPK1B	AZGP1	DUX4
KCND2	MATN3	ST6GALNAC1	GPR174	PLK5
CDY2B	VANGL1	KRT7	CSTA	PPP1R3G
OOEP	ST8SIA4	UGT2B7	F13A1	EXOC3L4
MX2	AGXT2L1	FXYD2	FMOD	NOSTRIN
UNC5A	GDF3	GSTA1	CLCA2	UPK3A
MS4A12	UCP1	C1orf116	ISLR	IHH
ACTN3	GPR64	ADH1B	SLC6A1	CDY1B
PHYHIP	EDA	MYEOV	EGR2	UNC93A
ST8SIA5	FREM1	GZMA	CYP21A2	C19orf80
ANKRD34B	KLF8	CEACAM3	MEOX1	LCN9
PHC1	IQCF5	PLA2G10	SERPINB2	PRAMEF11
DNAJA4	RTN4RL1	GAGE4	NR0B2	CDH17
IL18RAP	CCDC81	CYP2C19	FMO1	CASP5
DNMT3B	NMU	SIM1	PRG4	DNASE2B
MT1F	FOXN4	PTHLH	NUPR1	LGALS3
MAGEB1	PACSIN1	CFHR1	CALB2	CEL
GSC2	ZSWIM5	CD300A	PRSS1	CHAT
PPM1J	C17orf103	CDKN2B	C9orf24	OR51I1
VASH2	PEG10	CREB3L3	SPRR3	IL2RG
TRIM54	OR10H2	S100P	COL15A1	KLHL33
ADAMTS8	SORCS1	CAPN9	IL15RA	KLK1
TREX2	MCC	TSPAN1	CAPSL	NR1H4
OPRM1	OR10G7	TACSTD2	OR4A5	TFEC
CHST8	SPPL2C	DUOXA2	AGR3	IL22RA1
BNC1	MYCT1	INPP4B	LY96	GLP2R
DBC1	SH3BGR	CXCL5	PRLH	TNFSF18
GABRA5	TEX33	VTN	CD44	DUX2
NSG1	OR8K5	CFB	C11orf96	SPACA4
EGFL6	OXT	SEPP1	LSP1	KRTAP5-10
TRIM22	OR5M11	SERPINA4	CEBPD	OR1A1
GAGE8	C22orf42	S100A3	CXCL17	MSR1
NOTO	MAMLD1	IL31RA	HRASLS2	LYZL1

DYX1C1	S1PR3	IFI6	COL1A1	CLRN3
CASP10	VSIG4	WNT7A	S100P	FCER2
MT1M	MAGEB4	A4GNT	CFHR1	ARHGAP27
LHFPL4	PRDM1	ADAM28	GJB3	SLC9A3
ECHDC3	FAM159A	SPON2	IL8	PTCH2
SPATA31C1	C8B	CXCL1	CIB3	DQX1
FNDC7	HOMER2	GBP3	EGR1	SYBU
NMI	CCL2	RDH12	CHI3L1	GLTPD2
GFPT2	SBK2	ANXA4	S100A6	SVEP1
SYN1	RAB17	KRT35	GJB2	TMPRSS5
CLC	PRKCDBP	PHGR1	CYSLTR1	SLC6A8
KIF5A	ACOX3	ANXA8L2	WDR16	IL33
MMP17	PSKH2	HGD	OR8G5	KIAA1984
TMEM145	PLSCR4	C8orf47	DUSP2	MBD3L5
RABGAP1L	ARHGAP20	SLC28A3	TRIM77	LIPC
MS4A13	GRPR	KCNJ15	REG3A	CARD16
MT1E	SOX10	OMP	TNFAIP6	ARHGEF38
GAGE2E	ADAMTS5	HSFY2	COL12A1	CLEC3B
GABRP	ABCD1	MMP10	FAP	OBP2B
SYP	KCNG1	ARL14	NR2F1	CA6
ANKRD24	ERMN	MIA2	CPB1	SEMA3B
APCDD1L	GAS2L1	PDX1	ZG16B	LCN12
RAB3C	CD177	LGALS9B	BCL6	CD69
IL21	CLVS2	ANXA8	KCNJ15	DPP4
BEND4	PCDH10	KPNA7	TMPRSS4	FOXE3
CSH1	GABRB2	BLNK	FCER2	ALDH1L1
ZFP42	CAMKK2	DMBT1	MIA	KRTAP10-12
RTN4RL2	CXCR7	DUOX2	TP63	PIGZ
UGP2	SEMA5A	CEACAM6	NT5E	DHRS7C
OC90	PHACTR2	C3orf36	C11orf88	TFF3
FAM19A3	L1CAM	APCS	TGFB3	CXorf65
MATN4	PIK3R6	TYMP	GPR87	CPXM2
OPTC	C7orf57	SLC7A9	GBP2	CD300LG
ZMAT4	HLA-DQA1	VTCN1	KISS1	ISX
MEGF10	TMEM257	FAM3B	SRPX2	RBP4
CDHR1	SPANXN4	CA1	A4GNT	LCN1
GALNTL5	CALML5	FOXQ1	C4orf48	KRTAP5-6
APOBEC3B	MAGEA11	SI	BPIFB1	ACTRT2
TMEM151B	LEPREL1	UGT2B28	ADORA3	FAM13A
HSPA2	UTY	HR	KRT15	VIL1
GRIN2D	IL18R1	IL5RA	FOXD1	CA12
TMEM114	CFLAR	UGT1A3	CFB	PPP1R1B
HTR3A	OR52A1	SPDEF	CASP4	SLC26A3

GDPD2	LCE3B	CPA3	CCL11	PCP2
NLGN4X	TDGF1	CPB2	GAGE2C	CEBPA
NLGN4Y	IFNA6	DCDC2	EPHA3	GK2
PAH	RHOBTB3	TM4SF5	SMOC2	CD8B
CTF1	RET	CYSTM1	OBP2A	BPIFB2
CD200R1L	IL34	ABLIM3	S100A14	PPARG
NKX2-4	KRTAP9-8	NCF2	IGF2	C16orf90
SLC7A3	IRGC	GALNT5	SSTR4	SLAMF8
LHX8	FGF8	KRT6C	CXCL13	AFP
C5orf47	CCKBR	KRTAP2-3	TCF23	MYOM3
C7orf29	OVCH2	SLC26A3	MAL	PNLIPRP2
TACR3	GYPB	SMIM6	ANKRD30A	ACSS1
FAM65B	OR9Q2	ACER2	ECM1	LDB3
TPO	KIT	BCAS1	LRRC17	KRTAP5-9
RBP7	CLDN25	BAAT	AKR1C3	MUC12
PKLR	IER3	SPRR1B	APOA4	MYB
OXCT2	C9orf47	TRIM31	SOHLH1	SLC7A9
PPP1R17	ARL4D	LIPH	DUOXA2	ATP10B
FGF2	LRIG3	PLEKHS1	UGT1A6	SOWAHA
ARC	VRTN	VGLL1	AHNAK2	SOD3
NRXN1	ARMC7	KLK6	CMTM1	A1CF
CT45A4	ATP12A	ORM2	BPI	AQP12A
RASAL3	EGF	SGPP2	SIM2	HNF4A
CNTN1	AJAP1	CHRNA1	A2M	DEFB124
CPNE7	FCN2	KRTAP4-1	NKX6-2	HSPB3
C20orf141	BMP15	REG1B	PRB1	OR51A2
PIM2	NTN1	RHCG	ACTL7B	TMEM176B
SH2D3C	SAMD3	CXCL6	MMP1	TREH
KCNG3	ERBB4	MS4A8B	TMEM190	CDX1
C9orf135		C19orf77	KRTAP5-7	WNT11
HESX1		GDA	SP100	CIB4
CT45A2		CEACAM5	FOXC1	TMEM139
MAT1A		ZG16B	KLF4	CEACAM1
SLC4A9		KRT20	CAPS	GALNT9
VEPH1		RIPK3	EMP1	PTPRB
CHRNA6		LGALS9C	TSPO	KRTAP19-1
DPPA4		COL5A3	LURAP1L	FAM132A
SPATA22		SP100	CFH	PSG9
CXCL5		KRT23	TMEM171	POU4F1
L1TD1		RAMP1	CTRB2	MUC20
JAKMIP3		IL1A	PPP1R1B	FSCN2
GNA14		CASP4	HOPX	MST1R
DDX25		OR8U8	ONECUT3	S100A5

PIPOX	REG1A	SIGLEC12
PYGM	CCDC164	CA1
FDXR	OSR2	ADAD2
TLR3	SDPR	TRIM15
ATP8A2	C1R	CLPS
NMRK2	AREG	CYP4F12
GNAO1	CLIC6	CYP3A5
C9orf24	PCK1	MTTP
RHOH	OR4L1	OPN4
HCN4	S100A8	USH1C
SFRP2	HS3ST1	HSD17B2
TDRD12	CD70	KIR3DL1
HIST1H4F	HSPB6	REN
PRSS21	GHSR	CD97
ANKRD35	LAMB3	HNF1A
CBR1	CDC42EP5	OR2T27
GRM4	GPX2	INHA
PRUNE2	SPAG11A	INS
MOCOS	C20orf78	IL17RE
ACTRT3	SPAG11B	KRTAP10-5
STAC	KRT86	LGI4
ARHGAP22	ANXA10	
JPH4		
GRIN1		

Table S2. Overlapping genes when comparing d5/d10 organoids with publicly available data

Day 10 Program		Day 5 Program	
Wang (ileum)	Sherwood (ileum)	Wang (Duo)	Sherwood (Duo)
ANPEP	ABP1	ADAM28	AREG
CDH17	AFP	AKR1B10	DMBT1
CEACAM1	GUCA2A	ANXA10	GPR128
CHGA	PPP1R1B	BCAS1	ONECUT2
CLCA1	XPNPEP2	CLDN18	PDX1
CLRN3		CXCL17	SPP1
DPP4		CYP2C18	TM4SF4
FABP6		CYSTM1	
GPA33		MAOB	
GUCY2C		MSMB	
HEPACAM2		MUC1	
IL2RG		MYEOV	
LGALS2		NKX6-3	
LGALS3		PGC	
MEP1A		PLA2G10	
MUC17		PSCA	
MYO1A		RAB27B	
MYO7B		S100P	
NR1H4		SFTA2	
SLC17A4		SLC4A4	
SLC51A		SPINK1	
		TFF1	
		TFF2	
		TSPAN1	
		VSIG1	
		VSIG2	

p-values

	Day 10	Day 5
Wang Ileum	2.22E-16	5.02E-08
Wang Duo	0.014708928	1.00E-18
Sherwood Ileum	1.00E-18	2.55E-15
Sherwood duo	1.12E-05	1.00E-18

1E-18 is resolution of current analysis

Table S3. PCR primers

Gene	Sequence	Gene	Sequence
h-ABP1-F	TGCCCAAGTACCTGCTCTTT	h-IL2RG-F	CCACTCTGTGGAAGTGCTCA
h-ABP1-R	TCTGGTGGTAGATGCTGCTG	h-IL2RG-R	AGGTTCTTCAGGGTGGGAAT
h-ADAM28-F	CTGGAACGACTGTGGGTCTT	h-LGALS2-F	TCCACCATTGTCTGCAACTC
h-ADAM28-R	GCTCAGTGCTTTGTCCATCA	h-LGALS2-R	CAGGTAGCTCAGGTGGCTGT
h-AKR1B10-F	ATCACCGTTACGGCCTACAG	h-LGALS3-F	GCCTACCCATCTTCTGGACA
h-AKR1B10-R	CGTGCTGGTGTCACAGACTT	h-LGALS3-R	GTGGAAGGCAACATCATTCC
h-ANPEP-F	GGACCAAAGTAAAGCGTGGA	h-MAOB-F	GCGGATCTGGTCAAGTGAGT
h-ANPEP-R	GGCTGAGGGTGTAGTTGAGC	h-MAOB-R	CAGAGGGGGATTGAAGTGAA
h-ANXA10-F	GTCCTATGGGAAGCCTGTCA	h-MSMB-F	CCAGGAGATTCAACCAGGAA
h-ANXA10-R	GAGAACAATTGCAACCAGCA	h-MSMB-R	GTCCTTCTTCTCCACCACGA
h-AREG-F	ACCTACTCTGGGAAGCGTGA	h-MUC1-F	TTTTCTGGGCCTCTCCAATA
h-AREG-R	AGCCAGGTATTTGTGGTTCG	h-MUC1-R	CTGGGCAGAGAAAGGAAATG
h-CDH17-F	ACAATCGACCCACGTTTCTC	h-MUC17-F	ATAGGGCCACCGGAGACTAT
h-CDH17-R	GCTCCCGTTTTGTTGTTGAT	h-MUC17-R	TGCCAAGACGTAGCTTTGTG
h-CDX2-F	GGGCTCTCTGAGAGGCAGGT	h-MUC2-F	TGTAGGCATCGCTCTTCTCA
h-CDX2-R	GGTGACGGTGGGGTTTAGCA	h-MUC2-R	GACACCATCTACCTCACCCG
h-CLCA1-F	GCTGATGTTCTGGTTGCTGA	h-MYEOV-F	CCTAAATCCAGCCACGTCAT
h-CLCA1-R	CGTCAAATACTCCCCATCGT	h-MYEOV-R	CACCACGGAGACAATGACAC
h-CLDN18-F	TGTGGAACTCACTGCCTCAG	h-MYO7B-F	ACACGGAGATGGTGGAGAAG
h-CLDN18-R	CCAGGGACTTTCTGGTGGTA	h-MYO7B-R	GCAAACTTGGGGAAGGTGTA
h-CLRN3-F	AGGAACGACCCACAGTTACG	h-NKX6-3-F	TCTTTCTGCTTCTGGGGTGT
h-CLRN3-F	TAGATGCAACGCCAAAATGA	h-NKX6-3-R	GATCTTCTCGTCGTCCGAGT
h-CXCL17-F	CGCCCACTCTTCCAATTAAA	h-NR1H4-F	CCCCAAGTTCAACCACAGAT
h-CXCL17-R	GGGCACAGGCTAAGACTGAC	h-NR1H4-R	CTTTGATCCTCCCTGCTGAC
h-CYP2C18-F	CCGCATGGAGCTGTTTTTAT	h-OCT4-F	GTGGAGGAAGCTGACAACAA
h-CYP2C18-R	GAGAATTGCAGGTGACAGCA	h-OCT4-R	GGTTCTCGATACTGGTTCGC
h-CYSTM1-F	GTTCGTGGAGAGGAGAGGTG	h-ONECUT2-F	ATTCCCCCTATGTGGGTCTC
h-CYSTM1-R	CCAGCCGTACTGTGGGTATC	h-ONECUT2-R	CCACATGGGAACACTCCTCT
h-DMBT1-F	AGCACCAACCTGCTCTGTCT	h-OSR2-F	GTCAGGAGTGTGGGAAAGGA
h-DMBT1-R	GTCATTGTCTGCCTGCTTGA	h-OSR2-R	TCACAGTTTCGCCTGAACAC
h-DPP4-F	TCCCGGTGGGAGTACTATGA	h-PDX1-F	CGTCCGCTTGTTCTCCTC
h-DPP4-R	CAGGGCTTTGGAGATCTGAG	h-PDX1-R	CCTTTCCCATGGATGAAGTC
h-FABP6-F	GGCAAGTTCGAGATGGAGAG	h-PGC-F	TCCTGGTCCTTTTTGACACC
h-FABP6-R	TTGCTTTCCTTGCCAACAGT	h-PGC-R	CTGGATGCTCTGGACAGTCA
h-FOXA2-F	CGACTGGAGCAGCTACTATGC	h-PLA2G10-F	CTGGAACTGGCAGGAACTGT
h-FOXA2-R	TACGTGTTCATGCCGTTCAT	h-PLA2G10-R	GGAGTAGCGCTCTGTCTTGG
h-GAPDH-F	CTCTGCTCCTCCTGTTCGAC	h-PSCA-F	GGTTCCTGAGGCACATCCTA
h-GAPDH-R	TTAAAAGCAGCCCTGGTGAC	h-PSCA-R	CACAGGGTTAAGGGTGGAGA
h-GATA4-F	TCCAGAAGCCAGGACTAGGA	h-RAB27B-F	ACAGGTTCGAAGATGGGTTG
h-GATA4-R	TCAGCGTGTAAAGGCATCTG	h-RAB27B-R	ATGACCCCAAAAGTTCACCA
h-GUCA2A-F	GTAGCAACCCGAACTTTCCA	h-SFTA2-F	CCGGGTATGACTTTGCAACT
h-GUCA2A-R	TGCAGGAGAAAAGAGCTTCC	h-SFTA2-R	CCAAGAAGGACACAGGCTTC
h-GUCY2C-F	TGTGGTCACTGCTCTTCCAG	h-SOX17-F	CAGAATCCAGACCTGCACAA
h-GUCY2C-R	CAGTCACATTTAGGCCAGCA	h-SOX17-R	TCTGCCTCCTCCACGAAG
h-HOXB6-F	AAAAATCCCAAGGTCTGCAA	h-SPINK1-F	GCTGCCATGTGAAGAAGGAT
h-HOXB6-R	GCATAGCCCGACGAATAGAG	h-SPINK1-R	ACCGCACTTACCACGTCTCT
h-HOXB9-F	TAATCAAAGACCCGGCTACG	h-TFF2-F	ATGGATGCTGTTTCGACTCC
h-HOXB9-R	CTACGGTCCCTGGTGAGGTA	h-TFF2-R	CAGACTTCGGGAAGAAGCAC
h-HOXC8-F	TCCTGTGCGCTTTTATTGTG	h-TM4SF4-F	GGAAGCGGTGTCTTGATGAT
h-HOXC8-R	GCTGTCGGGACACAAAATCT	h-TM4SF4-R	TGAGGCATTTAGGACCCTTG
h-HOXC9-F	ACCGACAAGGAGCAGTCCTA	h-VSIG1-F	CTGATCCTAAGCTGCCTTGC
h-HOXC9-R	CCCAAATCGCAAGAGTTTTC	h-VSIG1-R	AGGCACGAGCTGTGAGAAAT
h-HOXD4-F	AATATCTGGCAGGGGCTCTC	h-XPNPEP2-F	CCTGGTATGGGGATCAGAGA
h-HOXD4-R	CTTCCATAGGGCCCTCCTAC	h-XPNPEP2-R	ACTGGCTCGAAGGTTGAAGA

Table S4. Antibodies and in situ probes

Antibody	Source	Dilution
CDX2	Bio-Genex, MU392A-UC	1:500
CHGA	Santa Cruz, sc-1488	1:100
DPP4	R&D systems, AF954	1:500
ECAD	BD Transduction Lab, 610181	1:500
ECAD	R&D systems, AF748	1:100
FABP2	Abcam, ab89195	1:100
FABP6	Santa Cruz, sc-23992	1:100
GATA4	R&D systems, AF 2606	1:100
KI67	Thermo Scientific Sp6 RM-9106-S1	1:400
LACTASE	Santa Cruz, sc-240614	1:100
MUC2	R&D systems, AF 1924	1:200
PDX1	Seven Hill, WRAB 1200	1:500
SI	Santa Cruz, sc-27603	1:100
STAB2	Santa Cruz, sc-81376	1:100
In Situ Probe	**Source**	
HS-ONECUT2	ACD-RNAscope®Probe, 473531	
HS-GUCA2A	ACD-RNAscope®Probe, 310621	
HS-DMBT1	ACD-RNAscope®Probe, 478711	